CMS Technical Summary Report #89-20

TRANSITIONAL WAVES FOR CONSERVATION LAWS

Eli L. Isaacson,
Dan Marchesin
and
Bradley J. Plohr

UNIVERSITY OF WISCONSIN

CENTER FOR THE MATHEMATICAL SCIENCES

Center for the Mathematical Sciences
University of Wisconsin—Madison
610 Walnut Street
Madison, Wisconsin 53705

December 1988

(Received December 7, 1988)

Sponsored by

U. S. Army Research Office
P. O. Box 12211
Research Triangle Park
North Carolina 27709

National Science Foundation
Washington, DC 20550

UNIVERSITY OF WISCONSIN - MADISON
CENTER FOR THE MATHEMATICAL SCIENCES

TRANSITIONAL WAVES FOR CONSERVATION LAWS *

Eli L. Isaacson [1]
Dan Marchesin [2]
Bradley J. Plohr [3]

CMS Technical Summary Report #89-20
December 1988

ABSTRACT

A new class of fundamental waves arises in conservation laws that are not strictly hyperbolic. These waves serve as transitions between wave groups associated with particular characteristic families. Transitional shock waves are discontinuous solutions that possess viscous profiles but do not conform to the Lax characteristic criterion; they are sensitive to the precise form of the physical viscosity. Transitional rarefaction waves are rarefaction fans across which the characteristic family changes from faster to slower. In this paper we identify an extensive family of transitional shock waves for conservation laws with quadratic fluxes and arbitrary viscosity matrices; this family comprises all transitional shock waves for a certain class of such quadratic models. We also establish, for general systems of two conservation laws, the generic nature of rarefaction curves near an elliptic region, thereby identifying transitional rarefaction waves. The use of transitional waves in solving Riemann problems is illustrated in an example where the characteristic and viscous profile admissibility criteria yield distinct solutions.

AMS (MOS) Subject Classification: 34D30, 35L65, 35L67, 35L80, 58F09

Key words: conservation laws, Riemann problems, non-strictly-hyperbolic, admissibility, viscosity, saddle-saddle connections, quadratic dynamical systems, line fields.

* Supported by the National Science Foundation under Grant No. DMS-8712058, the U. S. Army Research Office under Grant No. DAAL03-87-K-0028, the Financiadora de Estudos e Pesquisas, and the Conselho Nacional de Pesquisas.

[1] Department of Mathematics, P. O. Box 3036 Univ. Station, University of Wyoming, Laramie, WY 82071.

[2] Instituto de Matemática Pura e Aplicada and Pontifícia Universidade Católica, Rio de Janeiro, 22460 RJ, Brazil.

[3] Computer Sciences Department and Center for the Mathematical Sciences, University of Wisconsin-Madison, Madison, WI 53706.

TRANSITIONAL WAVES FOR CONSERVATION LAWS

Eli L. Isaacson, Dan Marchesin, and Bradley J. Plohr

1. Introduction

Non–strictly-hyperbolic systems of conservation laws possess fundamental wave solutions that are distinct from classical rarefaction and shock waves. These new waves are not associated with a particular characteristic family; rather they serve as transitions between classical wave groups. In the presence of such transitional waves, the solution of a Riemann problem for a system of n conservation laws can contain more than n wave groups. The purpose of the present paper is to study the character of transitional waves and the crucial role they play in solving Riemann problems.

For a particular model system of two conservation laws, Shearer, Schaeffer, Marchesin, and Paes-Leme [35] found it impossible to solve the general Riemann problem using only classical Lax shock waves. However, the general solution exists and is unique provided that a limited family of nonclassical discontinuities is allowed. For these crossing discontinuities, neither family of characteristics is compressive, in contrast to shock waves. The same type of discontinuity occurs in reactive gas dynamics as weak deflagration waves [5]. To solve another model system, Isaacson and Temple [21] utilized rarefaction waves that switch from characteristic family 2 to family 1 at the locus where eigenvalues coincide. Composite waves built from such discontinuities and rarefaction waves also arise [17, 14]. Thus the solution of a Riemann problem can involve waves that are not associated with a unique characteristic family. We view these examples as instances of a new class of waves, transitional waves. Thus a transitional shock wave is a crossing discontinuity that conforms to an admissibility criterion, and a transitional rarefaction wave changes from a faster family to a slower family. The nature of transitional shock and rarefaction waves is the subject of this paper.

As discussed in §2, we allow for any discontinuity that is the limit of traveling wave solutions of the conservation laws as augmented by a parabolic term; this is motivated by physical considerations. Admissible discontinuities correspond, then, to orbits connecting singularities of a dynamical system associated with the parabolic system. Whereas a classical shock wave generalizes to an orbit between a node and a saddle point, which is structurally stable under general perturbations, an admissible crossing discontinuity corresponds to a saddle-saddle connection, which has stringent stability restrictions. In

particular, the class of transitional shock waves depends critically on the viscous term in the parabolic equation. Furthermore, saddle-saddle connections signal bifurcations of admissible discontinuities. Also possible are waves corresponding to connecting orbits between nodes; however, these totally compressive waves can be decomposed into classical shock waves.

In §3 we study transitional shock waves for conservation laws with quadratic fluxes, which are simple models in which the new shock waves occur. The analysis is based on an explicit calculation that establishes a direct relationship between transitional shock waves and the viscous term: for a class of such quadratic models, a saddle-saddle connection must lie along a straight line parallel to a direction associated with the viscosity matrix. We provide a complete characterization of transitional shock waves of this form in §§3a-3c; circumstances under which these are the only transitional shock waves are established in §3c and App. A. As a consequence, the regions in state space where these waves play a role are easily identified. The case when the viscosity matrix is the identity, which is commonly assumed in analyses of traveling waves, is shown to have degenerate features.

In §4 we determine the behavior of rarefaction curves near a boundary between elliptic and hyperbolic behavior in a general system of two conservation laws. The transitional rarefaction waves are shown to arise from integral curves through isolated points on this boundary. The method of analysis represents both the 1- and 2-family rarefaction curves as a foliation defined by a single line field on a certain manifold. For strictly hyperbolic conservation laws, this manifold consists of two separate sheets, one for each family; in mixed-type problems, the two sheets are joined at the elliptic-hyperbolic boundary. Examples of these manifolds are given in App. B.

We illustrate the use of transitional waves to solve Riemann problems in §5. The essential construct is the transitional curve. The examples we study belong to a class of quadratic models for which the Riemann problem has a unique solution using only classical shock waves [20, 32]. We show, however, that some of the classical shock waves used in these solutions do not admit viscous profiles, and that transitional shock waves can be used in their place.

Finally, in §6, we summarize our results.

2. Transitional Waves

In this section we study the structure of solutions of Riemann problems. If the states in the initial data are close, the solution constructed classically consists of several groups of waves, each group corresponding to a characteristic family. Globally, however, the solution might contain transitional waves that interpolate between families, as we describe in §2a. To determine an appropriate class of transitional waves, we invoke the admissibility criterion based on viscous profiles; this criterion is discussed in §2b.

2a. Wave Groups

We are interested in solutions of a system of conservation laws

$$U_t + F(U)_x = 0 \tag{2.1}$$

governing the evolution, in one space dimension, of an n-dimensional state vector U. The function F is called the flux. The characteristic speeds for Eq. (2.1), *i.e.*, the eigenvalues of the Jacobian derivative matrix $F'(U)$, are denoted $\lambda_i(U)$, $i = 1, \ldots, n$. In the hyperbolic region, where the characteristic speeds are real, we order them as

$$\lambda_1(U) \leq \lambda_2(U) \leq \cdots \leq \lambda_n(U) \; . \tag{2.2}$$

The dependence of the characteristic speeds on U leads, in general, to focusing of waves and the formation of discontinuous solutions, so that Eq. (2.1) must be interpreted in the sense of distributions.

Much of the structure of general solutions of Eq. (2.1) is reflected in solutions that respect the invariance of the equation under the scaling transformation $(t, x) \mapsto (\alpha t, \alpha x)$. Such scale-invariant solutions satisfy the initial conditions of a Riemann problem: at $t = 0$, the solution U must be a constant U_L for $x < 0$ and another constant U_R for $x > 0$. Conversely, solutions of a Riemann problem are expected to be scale-invariant, *i.e.*, they depend on t and x only through the combination $\xi = x/t$. Although Riemann problems are only special initial value problems, the solutions of the general Cauchy initial value problem may be viewed as a nonlinear superposition of scale-invariant solutions [8].

A scale-invariant solution can be partitioned into several groups of waves; the waves in each group move together as a single entity. More precisely, we define a *wave group*

to be a scale-invariant solution that contains no intermediate constant states. Thus a solution of a Riemann problem comprises a sequence of wave groups moving apart from each other, as in Fig. 1(a). Wave groups are composed of two basic ingredients: centered rarefaction waves and centered discontinuous waves. [See Fig. 1(b).] A centered rarefaction wave associated with a characteristic family i is constructed using integral curves of the differential equation

$$\dot{U} = r_i(U) \ , \tag{2.3}$$

where $r_i(U)$ is a right eigenvector corresponding to $\lambda_i(U)$. A rarefaction wave corresponds to a segment of an integral curve along which $\lambda_i(U)$ is nondecreasing; it is defined by inverting the relation $\lambda_i(U) = \xi$. A centered discontinuous wave is a jump discontinuity that propagates at speed s and separates two constant states U_- and U_+, where U_-, U_+, and s satisfy the system of n equations

$$-s\,[U_+ - U_-] + F(U_+) - F(U_-) = 0 \ , \tag{2.4}$$

called the Rankine-Hugoniot jump condition. (By convention, U_- is on the left side of the discontinuity and U_+ is on the right side.)

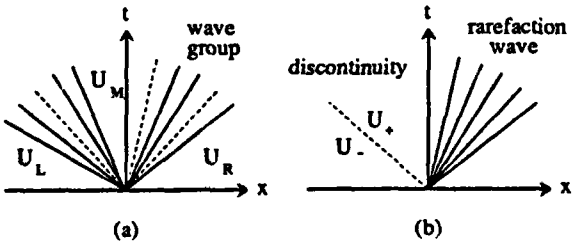

Fig. 1: Scale-invariant solutions: (a) a solution of a Riemann problem, comprising a sequence of wave groups; (b) a centered rarefaction wave and a centered discontinuous wave.

To avoid nonuniqueness of solutions of Riemann problems, the class of allowable discontinuous waves must be restricted. For conservation laws that are genuinely nonlinear,

Lax [25] introduced the admissibility requirement that the characteristics of one family impinge on both sides of the discontinuity, while the characteristics of the other families cross through the discontinuity. For more general conservation laws, characteristics must be permitted to become tangent to the discontinuity. Therefore we define a centered discontinuous wave to be a *Lax discontinuity* of the ith family provided that the characteristic speeds are related to the propagation speed as follows:

$$\lambda_i(U_+) \le s \le \lambda_i(U_-) \,, \tag{2.5}$$

$$\lambda_{i-1}(U_-) \le s \le \lambda_{i+1}(U_+) \,. \tag{2.6}$$

Remark: A Lax discontinuity is associated with a unique family except in one case: an ith-family discontinuity for which $\lambda_i(U_-) = s = \lambda_{i+1}(U_+)$ may be regarded also as associated with family $i+1$. This ambiguity in nomenclature, however, does not affect our results.

If we adopt the admissibility criterion based on characteristics and assume that all characteristic speeds are distinct, then any wave, *i.e.*, rarefaction wave or discontinuity, has an associated family. Observe that: (1) no wave can be preceded by a wave of a faster family; and (2) two waves of the same family must belong to the same wave group. Therefore a solution of a Riemann problem can contain at most n wave groups. In particular, no wave can appear strictly between a wave group containing an i-wave and another group containing an $(i+1)$-wave. These facts [26] generalize the classical picture [25] in which a solution of a Riemann problem consists of at most n shock or rarefaction waves, separated by constant states, where each wave is associated with a distinct family.

The characteristics criterion, however, is sometimes overly restrictive and other times too lax: a Riemann problem might have no solution or it might have many. An alternative admissibility criterion is to require discontinuous waves to possess viscous profiles, as described more fully in §2b. This is the viscosity admissibility criterion. In general, it is distinct from the characteristic criterion, since there exist Lax discontinuities that do not have viscous profiles, while some discontinuities with viscous profiles are not of Lax type. The viscosity criterion, too, can fail to guarantee existence and uniqueness of solutions of

Riemann problems, but we prefer it to the characteristic criterion because it derives from certain physical effects that have been neglected in the modeling equations. In this paper we adopt the viscosity admissibility criterion.

When discontinuities that are not of Lax type are allowed, or when characteristic speeds may coincide, it is possible for the solution of a Riemann problem to contain more than n wave groups. Consider, for example, a discontinuity satisfying

$$\lambda_i(U_-) < s < \lambda_{i+1}(U_-) \,, \tag{2.7}$$

$$\lambda_i(U_+) < s < \lambda_{i+1}(U_+) \,, \tag{2.8}$$

through which all characteristics cross. Such a *crossing discontinuity* can have a viscous profile, as we show in §3c. This wave can appear strictly between a wave group containing an i-wave and one containing an $(i+1)$-wave; see Fig. 2(a). As another possibility, an integral curve of family $i+1$ might pass tangent to the locus where $\lambda_{i+1}(U) = \lambda_i(U)$ and continue with an integral curve of family i (see §4). This gives a rarefaction wave that can lie strictly between i-waves and $(i+1)$-waves, as in Fig. 2(b).

In general, therefore, a distinct wave group can appear between one group containing an i-wave and another containing an $(i+1)$-wave. We call it an i,$(i+1)$-*transitional wave group*. A *transitional shock wave* is a crossing discontinuity that conforms to the viscosity admissibility criterion, and a *transitional rarefaction* wave is a rarefaction wave that changes from a faster family to a slower family. More complicated transitional wave groups are also possible. For example, a discontinuity satisfying $\lambda_i(U_-) < s = \lambda_{i+1}(U_-)$, as well as inequality (2.8), can adjoin an $(i+1)$-wave group on its left [17], as in Fig. 2(c). Similarly, a transitional rarefaction can adjoin an i-wave group on its right [see Fig. 2(d)] or an $(i+1)$-wave group on its left [14].

2b. Viscosity Admissibility Criterion

Typically, Eq. (2.1) is an approximation to an equation of the form

$$U_t + F(U)_x = \epsilon \left[D(U)\, U_x \right]_x \tag{2.9}$$

in the (singular) limit as $\epsilon \to 0^+$. Here D is the viscosity matrix, which models certain physical effects that are neglected in the conservation law. We require that the eigenvalues

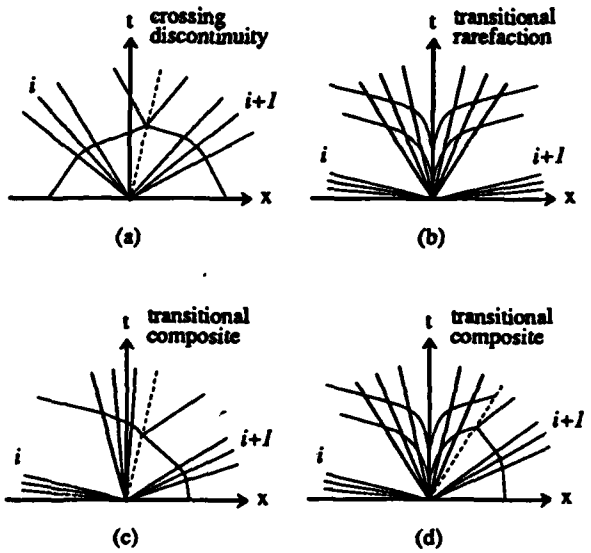

Fig. 2: Transitional waves: (a) a crossing discontinuity; (b) a transitional rarefaction wave; (c), (d) transitional composite waves. Light lines are characteristics.

of $D(U)$ have positive real part; this guarantees that short wavelength perturbations of constant solutions decay exponentially in time.

Physically realizable solutions of Eq. (2.1) are expected to be limits of solutions of the parabolic equation (2.9). In particular, certain centered discontinuous waves arise as limits of traveling wave solutions as follows. A traveling wave depends on t and x only through the combination $\xi = (x - st)/\epsilon$, and it approaches limits U_+ and U_- as $\xi \to \pm\infty$. Therefore Eq. (2.9) can be integrated once to obtain the dynamical system

$$-s\,[U(\xi) - U_-] + F(U(\xi)) - F(U_-) = D(U(\xi))\,\dot{U}(\xi)\ , \tag{2.10}$$

where the dot denotes differentiation with respect to ξ. Taking the limit of Eq. (2.10) as $\xi \to \infty$ shows that U_+, U_-, and s must be related by the Rankine-Hugoniot condition (2.4),

so that U_+ and U_- are critical points for the dynamical system. As $\epsilon \to 0^+$, the spatial region over which the solution makes the transition from U_- to U_+ shrinks to a point at $x = st$. Consequently, the traveling wave solution approaches a centered discontinuous wave. Thus a discontinuity is said to have a *viscous profile* when the dynamical system (2.10) has a connecting orbit flowing from U_- to U_+. It is natural to regard a discontinuity as admissible only if it has a viscous profile; this is the viscosity criterion for admissibility [5, 15, 7].

The critical points of a dynamical system are crucial to its study. For Eq. (2.10), a critical point is a state U_c that satisfies the Rankine-Hugoniot condition for the given state U_- and the speed s. The behavior of solutions in the neighborhood of a critical point U_c is reflected in qualitative features of solutions of the linearization of Eq. (2.10) about U_c:

$$[-s + F'(U_c)](U - U_c) = D(U_c)\dot{U} \ . \tag{2.11}$$

Such solutions are determined by the eigenvalues μ and corresponding eigenvectors $\hat{U}_\mu$ that satisfy

$$[-s + F'(U_c)]\hat{U}_\mu = \mu D(U_c)\hat{U}_\mu \ . \tag{2.12}$$

For example, $U = U_c + \Sigma_\mu c_\mu \exp(\mu\xi)\hat{U}_\mu$ when the eigenvalues are distinct. Thus the character of the critical point is determined by the eigenvalues μ.

Let us restrict now to systems of two conservation laws, so that Eq. (2.10) is a planar dynamical system. A critical point is classified as an antisaddle point (*i.e.*, a node, focus, or center) or as a saddle point. An orbit for the dynamical system connects either two saddle points, two antisaddle points, or a saddle and an antisaddle. To illustrate the relationship between the nature of critical points and the classification of discontinuities, we first discuss the case when D is the identity matrix; then the eigenvalues at a critical point U_c are $\mu_i = \lambda_i(U_c) - s$, $i = 1, 2$. This choice arises commonly in studies of viscous profiles for shock waves, but it is a degenerate case for crossing discontinuities, as we show in §3b.

A Lax shock wave of the first family has $s < \lambda_1(U_-) < \lambda_2(U_-)$ and $\lambda_1(U_+) < s < \lambda_2(U_+)$, so that the critical points U_- and U_+ of Eq. (2.10) are, respectively, a repelling node and a saddle point. Similarly, U_- and U_+ are, respectively, a saddle point and

an attracting node in the case of a Lax shock wave of the second family. Therefore an admissible discontinuity of Lax type corresponds to a saddle-node connection. For crossing discontinuities, which are defined by inequalities (2.7) and (2.8) with $i = 1$, the critical points U_- and U_+ are saddle points. Thus transitional shock waves correspond to saddle-saddle connections. Finally, a connecting orbit that joins a repelling node to an attracting node corresponds to a *totally compressive* shock wave:

$$\lambda_1(U_+) < s < \lambda_1(U_-) \,, \tag{2.13}$$

$$\lambda_2(U_+) < s < \lambda_2(U_-) \,, \tag{2.14}$$

so that the characteristics of both families impinge on the discontinuity.

In the general case when D is not a multiple of the identity matrix, the signs of $\lambda_i(U_c) - s$ do not always determine the character of a critical point U_c. Indeed, a critical point that is a node when $D = I$ can become a focus when D is changed. However, saddle points are preserved provided that the determinant of D is positive; this can be demonstrated as follows. Because μ_+ and μ_- are the eigenvalues of $D^{-1}\,[-s + F'(U_c)]$, their product $\mu_+\mu_-$ has the same sign as that of $(\lambda_+ - s)(\lambda_- - s)$, which is negative. Therefore μ_+ and μ_- must be real and have opposite sign. (Nodes, too, are preserved if the Jacobian matrix $F'(U_c)$ is symmetric and D is symmetric and positive definite, as shown in Lemma A.2, but this is a rather restrictive situation.)

When U_- and U_+ are sufficiently close, the saddle-antisaddle nature of Lax shock waves guarantees the existence and uniqueness of a connecting orbit [6, 4] (assuming strict hyperbolicity and genuine nonlinearity). This connecting orbit is expected to be structurally stable, in the sense that the orbit persists under small perturbations of U_-, U_+, and s [subject to the jump condition Eq. (2.4)] and under changes of the viscosity matrix D. By contrast, a connecting orbit between two saddle points is structurally unstable.

To be precise, structural stability holds if the dynamical system is Morse-Smale [12]. For example, the system is not Morse-Smale if some critical point is non-hyperbolic (the real part of an eigenvalue is zero) or if there is a saddle-saddle connection; in these cases bifurcation is expected. In the context of conservation laws, the critical point U_+ is non-hyperbolic if $\lambda_i(U_+) = s$ for some i, i.e., at boundaries between different types of discon-

tinuities. (These points are marked as dots in Fig. 3 below.) More generally, a boundary occurs if any critical point U_c, which corresponds to a discontinuity with speed s from U_- to U_c, has an eigenvalue μ with vanishing real part. In addition, bifurcation is expected if there is a saddle-saddle connection between two critical points. For instance, consider a 1-shock wave from U_- to U_+ such that an orbit connects another saddle point U_c to U_+; then U_+ can be a boundary between admissible 1-shock waves and inadmissible ones [34, 10]. (As discussed in §5, this occurs in Fig. 8, with U_-, U_+, and U_c being points L, C, and A_1.)

We see that saddle-saddle connecting orbits have two related roles in solving Riemann problems. The first is to cause bifurcations between admissible and inadmissible shock waves. The second is as transitional shock waves that appear in Riemann solutions. The structural instability of saddle-saddle connections indicates that only special crossing discontinuities should have viscous profiles. Thus the class of transitional shock waves is sensitive to the precise form of the parabolic terms in Eq. (2.9): if the solution of a Riemann problem contains a transitional shock wave, then the intermediate constant states in the solution are changed if the viscosity matrix is altered. In particular, a numerical method for solving conservation laws might select waves that are not physical if it relies on artificial viscosity. (This was emphasized to us by Schaeffer and Shearer [30].)

For completeness, we briefly describe the role of admissible totally compressive shock waves in Riemann problems. (We refer to Ref. [18] for an example of a system of conservation laws in which totally compressive waves arise; see also Ref. [32] for a discussion.) According to the inequalities (2.13) and (2.14), U_- and U_+ are both nodes, so that there is an infinite number of orbits connecting them. These inequalities also imply that a totally compressive wave cannot be preceded or followed by any other wave. In other words, there is only one wave group when a totally compressive wave occurs. Thus the utility of such waves for solving Riemann problems is limited: the set of right states $U_R = U_+$ for which the Riemann solution contains a totally compressive wave is one dimensional, comprising segments along the Hugoniot locus through $U_L = U_-$.

Let us presume that when U_R is perturbed from this set, a solution of the Riemann problem with data U_L and U_R exists and depends L^1_{loc}-continuously on U_R. Then the

perturbed solution must contain a 1-wave group with a 1-shock wave on its left and a 2-wave group with a 2-shock wave on its right, with shock speeds approximately the same as that of the totally compressive wave. In the limit as U_R moves back onto the segment of totally compressive waves, the critical points corresponding to the Lax shock waves remain joined by orbits. In particular, the dynamical system for the totally compressive wave must contain other critical points besides U_- and U_+: the repelling node U_- is also connected to a saddle point, and a saddle point connects to the attracting node U_+. From this perspective, a totally compressive wave should be regarded as containing 1- and 2-shock waves, not as a new type of shock wave.

3. Transitional Shock Waves in Quadratic Models

In this section, we examine crossing discontinuities that possess viscous profiles. These profiles correspond to saddle-saddle connecting orbits for the dynamical system (2.10). Our results are limited to systems of two conservation laws with quadratic fluxes, which are described in §3a. Nevertheless, we believe that the results reflect the structure of transitional shock waves for general systems of two conservation laws. (See §5 for further discussion.)

The motivation for our analysis derives from the theory of polynomial dynamical systems in the plane: for certain quadratic systems, a saddle-saddle connecting orbit must be a straight line segment. In §3b, therefore, we determine conditions under which a discontinuity (not necessarily a crossing discontinuity) possesses a viscous profile that lies along a straight line. Then, in §3c, we state sufficient conditions for a quadratic model to have the property that a viscous profile for a crossing discontinuity must be a straight line segment.

3a. Quadratic Models

A quadratic model is a system of two conservation laws

$$U_t + F(U)_x = 0 \tag{3.1}$$

in which the flux is a quadratic function: writing $U = (u, v)^{\mathrm{T}}$ and $F = (f, g)^{\mathrm{T}}$,

$$f(u,v) = \tfrac{1}{2}(a_1 u^2 + 2b_1 uv + c_1 v^2) + d_1 u + e_1 v \ , \tag{3.2}$$

$$g(u,v) = \tfrac{1}{2}(a_2u^2 + 2b_2uv + c_2v^2) + d_2u + e_2v \ . \tag{3.3}$$

Evidently, a quadratic flux approximates the flux for a general system of two conservation laws in the neighborhood of a point. When the linear terms are absent, the two characteristic speeds coincide at $U = 0$; more generally, any (nondegenerate) quadratic model fails to be strictly hyperbolic somewhere in the u-v plane. Furthermore, *elliptic regions*, where the characteristic speeds are complex, might occur. The Riemann problem for quadratic models has been studied by Gomes, H. Holden, L. Holden, Isaacson, Marchesin, Paes-Leme, Plohr, Rascle, Schaeffer, Serre, Shearer, and Temple [19, 31, 35, 18, 20, 21, 13, 29, 33, 32, 10, 14, 34].

In the study of Riemann problems, the solutions of the Rankine-Hugoniot condition (2.4) play an important role. For systems of two conservation laws, it is convenient to eliminate the speed s from the Rankine-Hugoniot condition. With $U_0 = U_-$ regarded as fixed, this yields a single equation for states $U = U_+$ in the *Hugoniot locus* of U_0:

$$H_{(u_0,v_0)}(u,v) = 0 \ , \tag{3.4}$$

where

$$H_{(u_0,v_0)}(u,v) = (u-u_0)\,[g(u,v) - g(u_0,v_0)] - (v-v_0)\,[f(u,v) - f(u_0,v_0)] \tag{3.5}$$

is the Hugoniot function. Similarly, the shock speed s is given by

$$s = \frac{(u-u_0)\,[f(u,v) - f(u_0,v_0)] + (v-v_0)\,[g(u,v) - g(u_0,v_0)]}{(u-u_0)^2 + (v-v_0)^2} \ . \tag{3.6}$$

An example of a Hugoniot locus is drawn in Fig. 3. For quadratic models, H is a cubic polynomial in the two variables u and v. Moreover [18], the Hugoniot locus of U_0 is parameterized by angle in the polar coordinate system centered at U_0, except when the Hugoniot locus contains a line through U_0. To explain this result, we first introduce some convenient notation and terminology.

Associated to a given quadratic model are the functions α, β, γ, and $\tilde{\alpha}$, $\tilde{\beta}$, $\tilde{\gamma}$, which are defined by

$$\alpha(\varphi) = \tfrac{1}{2}\{(a_2+b_1)\cos 2\varphi + (b_2-a_1)\sin 2\varphi + a_2 - b_1\} \ , \tag{3.7}$$

$$\beta(\varphi) = \tfrac{1}{2}\{(b_2+c_1)\cos 2\varphi + (c_2-b_1)\sin 2\varphi + b_2 - c_1\} \ , \tag{3.8}$$

$$\gamma(\varphi) = \tfrac{1}{2}\{(d_2+e_1)\cos 2\varphi + (e_2-d_1)\sin 2\varphi + d_2 - e_1\} \ , \tag{3.9}$$

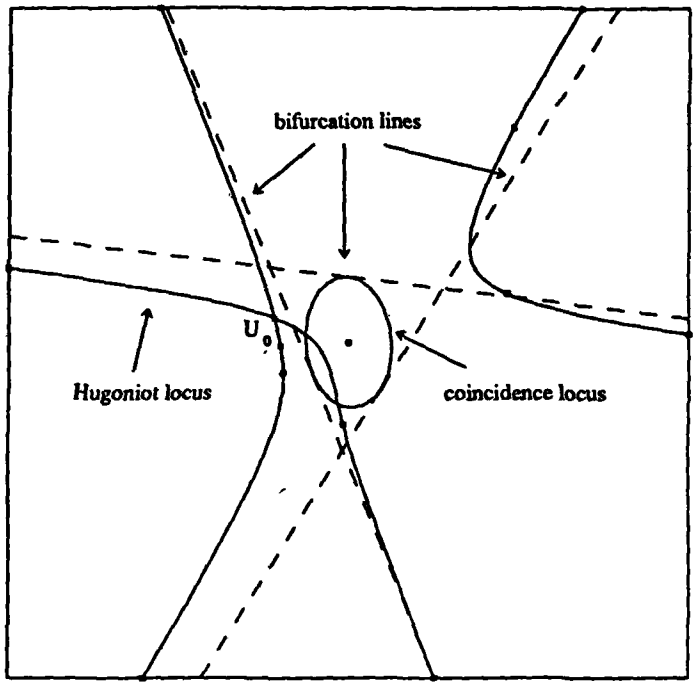

Fig. 3: Bifurcation lines for a quadratic model, and the Hugoniot locus for a representative point U_0. Dots along the Hugoniot locus demarcate segments with different shock types. Also shown is the coincidence locus, where the characteristic speeds coincide; inside of this curve, the system is elliptic.

and

$$\tilde{\alpha}(\varphi) = \tfrac{1}{2}\{(a_1 - b_2)\cos 2\varphi + (b_1 + a_2)\sin 2\varphi + a_1 + b_2\}\ , \tag{3.10}$$

$$\tilde{\beta}(\varphi) = \tfrac{1}{2}\{(b_1 - c_2)\cos 2\varphi + (c_1 + b_2)\ \sin 2\varphi + b_1 + c_2\}\ , \tag{3.11}$$

$$\tilde{\gamma}(\varphi) = \tfrac{1}{2}\{(d_1 - e_2)\cos 2\varphi + (e_1 + d_2)\sin 2\varphi + d_1 + e_2\}\ . \tag{3.12}$$

If we set $U = U_0 + R(\cos\varphi, \sin\varphi)^{\mathrm{T}}$, then the Hugoniot function is

$$H_{(u_0,v_0)}(u,v) = R^2\left\{\tfrac{1}{2}R\big[\alpha(\varphi)\cos\varphi + \beta(\varphi)\sin\varphi\big] + \alpha(\varphi)u_0 + \beta(\varphi)v_0 + \gamma(\varphi)\right\}\ ; \tag{3.13}$$

moreover,

$$s = \tfrac{1}{2}R\big[\tilde{\alpha}(\varphi)\cos\varphi + \tilde{\beta}(\varphi)\sin\varphi\big] + \tilde{\alpha}(\varphi)u_0 + \tilde{\beta}(\varphi)v_0 + \tilde{\gamma}(\varphi)\ . \tag{3.14}$$

An angle φ is called an *asymptotic angle* when

$$\alpha(\varphi)\cos\varphi + \beta(\varphi)\sin\varphi = 0\,, \tag{3.15}$$

and it is called a *characteristic angle* for a given state U_0 when

$$\alpha(\varphi)u_0 + \beta(\varphi)v_0 + \gamma(\varphi) = 0\,. \tag{3.16}$$

The set of states U_0 satisfying Eq. (3.16) constitutes the *characteristic line* $\mathcal{L}(\varphi)$ associated with φ. At points along such a line, one of the eigenvectors has inclination angle φ. The characteristic line associated with an asymptotic angle is called a *bifurcation line* (see Fig. 3). Notice that asymptotic angles and bifurcation lines depend solely on the coefficients defining the model, not on U_0. We remark that the envelope of the characteristic lines is the coincidence locus, *i.e.*, points where the eigenvalues coincide; this is demonstrated in App. B.1. In particular, bifurcation lines are tangent to the coincidence locus.

The parameterization of Hugoniot loci is a consequence of Eq. (3.13):

Proposition 3.1 ([18]):

(a) Suppose that φ is not an asymptotic angle. Then the line through U_0 at angle φ intersects the Hugoniot locus of U_0 at a state $U \neq U_0$ if and only if φ is not a characteristic angle for U_0.

(b) Suppose that φ is an asymptotic angle. Then the line through U_0 at angle φ intersects the Hugoniot locus of U_0 at a state $U \neq U_0$ if and only if U_0 lies on the bifurcation line associated with φ, in which case the Hugoniot locus contains this line.

Remarks:

(1) If U_0 belongs to the hyperbolic region, the Hugoniot locus through U_0 has two branches; these branches are tangent at U_0 to the right eigenvectors of $F'(U_0)$. According to Eq. (3.13), then, $(\cos\varphi, \sin\varphi)^{\mathrm{T}}$ is a right eigenvector if and only if φ is a characteristic angle for U_0. By Eq. (3.14), the corresponding eigenvalue is $\lambda = \tilde{\alpha}(\varphi)u_0 + \tilde{\beta}(\varphi)v_0 + \tilde{\gamma}(\varphi)$.

(2) The Hugoniot locus approaches infinity at the asymptotic angles (as in Fig. 3). Eq. (3.15) is a cubic equation for $\tan\varphi$, so that generically the number of bifurcation lines is one or three.

(3) The Hugoniot locus for a state U_0 has a secondary bifurcation point if and only if U_0 lies on a bifurcation line, in which case the secondary bifurcation occurs on this line.

(4) For later purposes (see Lemma 3.4), we note that

$$\alpha(\varphi)\cos\varphi + \beta(\varphi)\sin\varphi = (-\sin\varphi, \cos\varphi)F''(0)\cdot\begin{pmatrix}\cos\varphi\\ \sin\varphi\end{pmatrix}^2 \tag{3.17}$$

and

$$\tilde{\alpha}(\varphi)\cos\varphi + \tilde{\beta}(\varphi)\sin\varphi = (\cos\varphi, \sin\varphi)F''(0)\cdot\begin{pmatrix}\cos\varphi\\ \sin\varphi\end{pmatrix}^2 . \tag{3.18}$$

When studying viscous profiles for quadratic models, we take the viscosity matrix D to be constant; this is reasonable because quadratic models arise as expansions. Then Eq. (2.10) becomes the planar, autonomous system of ordinary differential equations

$$D\,\dot{U}(\xi) = -s\,[U(\xi) - U_-] + F(U(\xi)) - F(U_-)\,. \tag{3.19}$$

3b. Viscous Profiles

A viscous profile for a crossing discontinuity is defined by an orbit that joins two saddle points. For dynamical systems that are quadratic gradients, Chicone [2] has shown that every saddle-saddle connection is a straight line segment. With this in mind, we first construct all discontinuities (not necessarily crossing discontinuities) that have straight-line orbits. This approach yields a large class of transitional shock waves, as discussed in the next subsection.

For convenience, we use the notation $\overline{U} = \frac{1}{2}(U_+ + U_-)$ for the average of, and $\Delta U = U_+ - U_-$ for the difference between, two states U_+ and U_-. The construction relies on an obvious property of quadratic functions.

Lemma 3.2: *Suppose Q is a quadratic function such that $Q(U_+) = Q(U_-)$. Then*

$$Q(\overline{U} + \rho\Delta U) = Q(\overline{U}) + \tfrac{1}{2}\rho^2 Q''(\overline{U})\cdot(\Delta U)^2\ . \tag{3.20}$$

Proposition 3.3: *Let F be quadratic, and suppose that s, U_-, and $U_+ \neq U_-$ satisfy the Rankine-Hugoniot condition (2.4). Then the straight line segment between U_- and U_+ is a connecting orbit for Eq. (3.19) if and only if there is a constant $\mu \neq 0$ such that*

$$\mu D \Delta U = \tfrac{1}{2} F''(0) \cdot (\Delta U)^2 \ . \tag{3.21}$$

The orbit is traversed from U_- to U_+ if and only if $\mu < 0$.

Proof: An orbit connecting U_- and U_+ along a line takes the form

$$U(\xi) = \overline{U} + \rho(\xi) \Delta U \tag{3.22}$$

with $-\frac{1}{2} < \rho(\xi) < \frac{1}{2}$. If the quadratic function Q in Lemma 3.2 is defined by $Q(U) = -s(U - U_-) + F(U) - F(U_-)$, then the dynamical system (3.19) becomes $D\dot{U} = Q(U)$, *i.e.*,

$$\dot{\rho} D \Delta U = Q(\overline{U}) + \tfrac{1}{2} \rho^2 Q''(\overline{U}) \cdot (\Delta U)^2 \ . \tag{3.23}$$

But $0 = Q(U_-) = Q(\overline{U}) + \frac{1}{8} Q''(\overline{U}) \cdot (\Delta U)^2$ and $Q''(\overline{U}) = F''(0)$, so

$$\dot{\rho} D \Delta U = \tfrac{1}{2} \left(\rho^2 - \tfrac{1}{4}\right) F''(0) \cdot (\Delta U)^2 \ . \tag{3.24}$$

This equation is satisfied if Eq. (3.21) holds and

$$\dot{\rho} = \mu \left(\rho^2 - \tfrac{1}{4}\right) \ . \tag{3.25}$$

Provided that $\mu \neq 0$, Eq. (3.25) has a solution with ρ varying between $-\frac{1}{2}$ and $\frac{1}{2}$. Conversely, if ρ parameterizes a connecting orbit along a straight line, Eq. (3.24) shows that Eq. (3.25) must hold for some $\mu \neq 0$, and therefore that Eq. (3.21) is satisfied. The parameter ρ increases from $-\frac{1}{2}$ to $\frac{1}{2}$, *i.e.*, the orbit is traversed from U_- to U_+, if and only if $\mu < 0$. □

The quantity μ is related to the eigenvalues for the linearized differential equations at the critical points, as we now show. Suppose that the straight line segment from U_- to U_+ is an orbit; then it must coincide with an unstable manifold for U_- and a stable manifold for U_+. Therefore, by Eq. (2.12),

$$[-s + F'(U_\pm)] \Delta U = \mu_\pm D \Delta U \tag{3.26}$$

with $\mu_+ \le 0 \le \mu_-$. Subtracting these two equations yields

$$[F'(U_+) - F'(U_-)]\,\Delta U = (\mu_+ - \mu_-) D\,\Delta U\ . \tag{3.27}$$

Since $F'(U_+) - F'(U_-) = F''(0)\,\Delta U$, we obtain Eq. (3.21) with $\mu = \frac{1}{2}(\mu_+ - \mu_-) \le 0$. Moreover, adding Eqs. (3.26) shows that

$$\left[-s + F'(\overline{U})\right]\Delta U = \tfrac{1}{2}(\mu_+ + \mu_-) D\,\Delta U\ . \tag{3.28}$$

According to the midpoint rule for quadratic models [18], the left-hand side vanishes when U_-, U_+, and s satisfy the Rankine-Hugoniot condition:

$$s\,\Delta U = F(U_+) - F(U_-) = \int_{-1/2}^{1/2} F'(\overline{U} + \rho\Delta U)\Delta U\, d\rho = F'(\overline{U})\Delta U\ . \tag{3.29}$$

Consequently, $\mu_+ + \mu_- = 0$, so that $\mu = \mu_+ = -\mu_-$.

As the next lemma shows, solutions of Eq. (3.21) are related to the asymptotic angles for the quadratic model with the flux function $D^{-1}F$. Because these angles are determined by the viscosity matrix D, as well as by F, we call them *viscosity angles*. Also, the characteristic line $\mathcal{L}(\varphi)$ associated with a viscosity angle is called a *viscosity line*.

Lemma 3.4: *Let U_+ lie on the line through U_- at angle φ, with $U_+ \neq U_-$. Then Eq. (3.21) holds for some μ if and only if φ is a viscosity angle.*

Proof: Let $\Delta U = R(\cos\varphi, \sin\varphi)^{\mathrm{T}}$. Then Eq. (3.21) holds for some μ if and only if

$$0 = (-\sin\varphi, \cos\varphi) D^{-1} F''(0) \cdot \begin{pmatrix} \cos\varphi \\ \sin\varphi \end{pmatrix}^2\ . \tag{3.30}$$

Comparing this with Eq. (3.17), we see that Eq. (3.21) holds if and only if φ is an asymptotic angle for the quadratic model with flux $D^{-1}F$. □

The existence of straight-line orbits depends also on the eigenvalue μ. To determine a formula for μ, suppose that φ is a viscosity angle and that U_+ lies on the line through U_- at angle φ, say $U_+ = U_- + R(\cos\varphi, \sin\varphi)^{\mathrm{T}}$. Then Eqs. (3.21) and (3.18) imply that

$$\mu = \tfrac{1}{2} R\left[\tilde{\alpha}_D(\varphi)\cos\varphi + \tilde{\beta}_D(\varphi)\sin\varphi\right]\ ; \tag{3.31}$$

here $\tilde{\alpha}_D$ and $\tilde{\beta}_D$ are the functions associated with $D^{-1}F$ that are defined (for F) in Eqs. (3.10) and (3.11). A viscosity angle φ is said to be *exceptional* if $\tilde{\alpha}_D(\varphi)\cos\varphi + \tilde{\beta}_D(\varphi)\sin\varphi = 0$: no straight-line profiles are possible at an exceptional viscosity angle because $\mu = 0$. Otherwise, if φ is not exceptional, then the sign of μ is determined by the sign of R. Thus $\mu < 0$ on a particular open ray with respect to U_-. For simplicity, we say that U_+ is *correctly oriented* with respect to U_- along the viscosity line if it lies in this ray.

The construction of discontinuities with straight-line profiles proceeds as follows. The line at each viscosity angle is drawn through U_0, and its intersection U with the Hugoniot locus through U_0 is found; then U and U_0 are joined by a profile along this direction. Of course, this intersection might not exist; the precise conditions are consequences of the characterization of Hugoniot loci given in Prop. 3.1.

Theorem 3.5: *Assume that the viscosity matrix D is invertible, and consider a fixed viscosity angle φ for D that is not exceptional. Let $\mathcal{L}(\varphi)$ be the viscosity line associated with φ.*

(a) Suppose that φ is not an asymptotic angle. Then U_0 is connected to some $U \neq U_0$ on the Hugoniot locus of U_0 by a connecting orbit lying along a straight line at angle φ if and only if $U_0 \notin \mathcal{L}(\varphi)$. In this case, the corresponding state U is unique.

(b) Suppose that φ is an asymptotic angle. (Thus $\mathcal{L}(\varphi)$ is a bifurcation line.) Then U_0 is connected to some $U \neq U_0$ on the Hugoniot locus of U_0 by a connecting orbit lying along a straight line at angle φ if and only if $U_0 \in \mathcal{L}(\varphi)$. In this case, the corresponding states U comprise all of $\mathcal{L}(\varphi)$.

The connecting orbit is traversed from U_0 to U if and only if U is correctly oriented with respect to U_0.

Part (a) of this theorem is illustrated in Fig. 4, which shows three discontinuities that possess straight-line profiles. Part (b) is nongeneric, but it arises when D is a multiple of the identity, which is the simplest choice. Bifurcations of saddle-saddle connections under cubic perturbations has been studied in the case $D = I$ in Ref. [36].

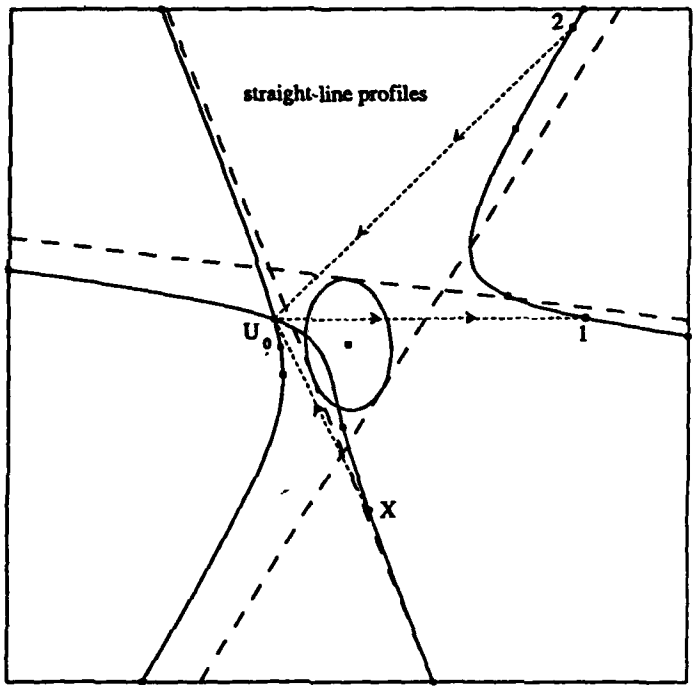

Fig. 4: Discontinuities with straight-line profiles. The dashed lines are drawn through U_0 at the viscosity angles; arrows indicate the direction of the connecting orbit. The discontinuity corresponding to point X is of crossing type, while point 1 is the right state of a 1-shock and point 2 is the left state of a 2-shock.

3c. Saddle-Saddle Connecting Orbits

Theorem 3.5 characterizes when a discontinuity in a quadratic model possesses a straight-line profile. To apply it to solving Riemann problems, we must account for the wave type of the discontinuity, *i.e.*, the relationships between the propagation speed and the characteristic speeds on the two sides of the discontinuity. Indeed, Theorem 3.5 allows a discontinuity with a straight-line profile to be of either Lax or crossing type. Lax discontinuities with straight-line profiles, however, constitute only a small subset of the Lax discontinuities with viscous profiles. This is because saddle-node connecting orbits are structurally stable. By contrast, profiles for crossing discontinuities, which correspond

to saddle-saddle connecting orbits, do not persist when the discontinuity suffers a generic perturbation.

In this subsection, we describe the set of crossing discontinuities with straight-line profiles. Furthermore, for certain classes of quadratic models, we show that the only crossing discontinuities with viscous profiles take the form constructed in Theorem 3.5. Within these classes, therefore, the set of points (U_L, s, U_R) corresponding to transitional shock waves has codimension 3, whereas the set corresponding to Lax shock waves has codimension 2.

Assume that the hypotheses of Theorem 3.5 hold. In both cases (a) and (b), any point U_0 in a certain set is connected to some $U \neq U_0$ by a straight-line profile at angle φ. We define the *transitional region* for the viscosity angle φ to be the subset of points U_0 for which at least one of these discontinuities is of crossing type. Thus the transitional region is defined by the inequalities

$$\lambda_1(U_0) < s < \lambda_2(U_0) \,, \tag{3.32}$$

$$\lambda_1(U) < s < \lambda_2(U) \,, \tag{3.33}$$

and the requirement of being correctly oriented. In the situation of part (a), the transitional region is an open subset of the plane, and to each of its points corresponds a unique admissible crossing discontinuity for φ. In fact, the transitional region is a wedge, as we show presently. This generic case is illustrated in Fig. 5. Similarly, for part (b), the transitional region is a ray of the bifurcation line $\mathcal{L}(\varphi)$, and to each point in this set corresponds an open interval of admissible crossing discontinuities.

The precise form of the boundary of the transitional region is determined as follows. We consider a particular viscosity angle φ and allow the point U_0 to vary; the corresponding point $U = U_0 + R(\cos\varphi, \sin\varphi)^{\mathrm{T}}$ is joined to U_0 by a straight-line profile. The boundary of the transitional region consists of points U_0 for which some of the inequalities (3.32) and (3.33) becomes equalities, so that the speed of the shock coincides with the characteristic speed at either the left or right state: $\det[-s + F'(U_c)] = 0$, with U_c being U_0 or U. By Eqs. (3.13) and (3.14) each of these two equations is quadratic in u_0 and v_0. Points U_0 on the viscosity line satisfy these equations, so that each equation factors into

a product of linear polynomials; *i.e.*, each solution set is a pair of crossed lines. Notice, however, that the solutions on the viscosity line are irrelevant because $R = 0$ along this line. We conclude that the boundary of the transitional region is contained in two crossed lines. One ray of each line corresponds to profiles that are correctly oriented, so that the transitional region is a wedge. In the case of part (b), the wedge collapses to a single ray.

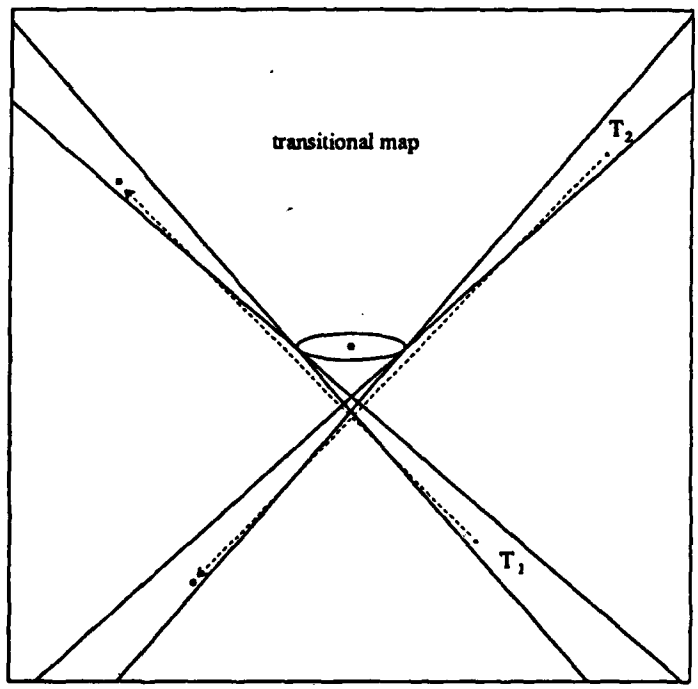

Fig. 5: Transitional regions. A point in region T_1 or T_2 is the left state for a transitional shock wave. The corresponding right state is given by the transitional map indicated by the dashed lines, which lie at viscosity angles. One of the three viscosity angles does not lead to transitional shock waves, so that there is no corresponding transitional region.

We now turn attention to the question of whether all saddle-saddle connections are straight line segments, so that the transitional shock waves constructed above are the only ones. This is true for certain classes of quadratic models and certain choices for the viscosity matrix. Some of the results that we describe concern quadratic models that are

strictly hyperbolic except at $U = 0$. Schaeffer and Shearer [31] have classified such models; they show that a linear change of dependent variables U brings the system of conservation laws to a normal form in which the flux is a gradient, *i.e.*, $F(U) = C'(U)$. The qualitative structure of solutions falls into four categories, corresponding to four regions in parameter space, which are labeled Cases I–IV.

When the flux is a gradient, the vector field on the right-hand side of the dynamical system (3.19) is also a gradient: with G defined by

$$G(u,v) = C(u,v) - C(u_-,v_-) - \tfrac{1}{2}s\left[(u-u_-)^2 + (v-v_-)^2\right] - f(u_-,v_-)(u-u_-) - g(u_-,v_-)(v-v_-)\ , \tag{3.34}$$

viscous profiles satisfy

$$D\,\dot{U}(\xi) = G'(U(\xi))\ . \tag{3.35}$$

In particular, when the viscosity matrix D is a multiple of the identity matrix, the dynamical system (3.35) is a quadratic gradient system in the plane. Such systems have been studied in connection with Hilbert's 16th problem (see, *e.g.*, Chicone and Jinghuang [3]). The following result of Chicone [2] bears directly on our application:

Theorem 3.6 (Chicone): *For a quadratic gradient system in the plane, an orbit connecting two saddle points is a straight line segment.*

Notice that when D is a multiple of the identity matrix, viscosity angles coincide with asymptotic angles. Therefore part (b) of Theorem 3.5 yields the following.

Corollary 3.7: *Suppose that the flux for a quadratic model is a gradient. Then if the viscosity matrix D is a multiple of the identity matrix, any viscous profile for a crossing discontinuity must lie along a straight line. Furthermore, a crossing discontinuity connecting U_- to U_+ has a viscous profile if and only if U_- and U_+ both lie on the same bifurcation line and U_+ is correctly oriented with respect to U_-.*

For general choices of D, however, viscosity angles differ from asymptotic angles, so that part (a) of Theorem 3.5 applies instead. The class of discontinuities with straight-line profiles then takes a different form: for each state U_- in a certain open set, there is a finite set of states U_+ corresponding to such discontinuities. In this sense, the case when D is

a multiple of the identity matrix is not representative of the generic case. Extension of Corollary 3.7 to more general viscosity matrices requires generalizing Chicone's Theorem. Recently, Gomes [9, 11] has proved one such generalization:

Theorem 3.8 (Gomes): *Consider a quadratic dynamical system in the plane such that there are more than two critical points at infinity. If two saddle points are connected by an orbit, then the straight line segment joining them is also an orbit. Moreover, if the saddle points are connected by an orbit distinct from the straight line segment, then the region bounded by these orbits contains a critical point for which the eigenvalues are not real. In particular, if all critical points in the finite plane have real eigenvalues, then any orbit connecting two saddle points is a straight line segment.*

Based on this result and part (a) of Theorem 3.5, we can extend Corollary 3.7 to allow for symmetric, positive definite viscosity matrices, provided that there is more than one viscosity angle.

Corollary 3.9: *Suppose that the flux for a quadratic model is a gradient and that the viscosity matrix D is symmetric and positive definite. Suppose also that there is more than one viscosity angle. Then any viscous profile for a crossing discontinuity must lie along a straight line.*

Proof: See App. A. □

We emphasize, however, that for some quadratic models, saddle-saddle connecting orbits need not be straight line segments. Azevedo [1] has given such an example: for a certain quadratic model with an elliptic region, U_- and U_+ can be chosen so that there is a curved saddle-saddle connecting orbit from U_+ to U_- in addition to a straight-line orbit from U_- to U_+. This is possible because there is a critical point, located in the elliptic region, that is a center. There can be up to three orbits connecting two saddle points in a quadratic dynamical system.

Theorem 3.8 shows that the features observed in this example are true more generally: if two saddle points are connected by a curved orbit, then they are joined also by a straight-line connection oriented in the opposite direction. In particular, the set of transitional shock waves with curved saddle-saddle connections has higher codimension than has the set

with straight-line connections. Therefore, the following results hold for general quadratic conservation laws and viscosity matrices such that there is more than one viscosity angle: the left and right states of a transitional shock wave must lie along a line parallel to a viscosity line, so that such a wave is characterized by Theorem 3.5; and transitional shock waves generically have straight-line profiles and arise from the transitional map described above.

4. Transitional Rarefaction Waves

In this section, we study transitional rarefaction waves for systems of two conservation laws. Such a wave arises when an integral curve of family 2 is followed by an integral curve of family 1 (in the direction of increasing characteristic speed). Of necessity, the two characteristic speeds coincide at the point where these curves join. Suppose that the set of states U at which $\lambda_1(U) = \lambda_2(U)$ forms a smooth curve separating a hyperbolic region from an elliptic region. (Models for which the coincidence locus separates two regions of strict hyperbolicity are possible also; one example is discussed in §B.2.) Fig. 6 illustrates four conceivable configurations of rarefaction curves in the vicinity of this curve. Transitional rarefaction waves occur in Figs. 6(b) and 6(d), while in Figs. 6(a) and 6(c) they do not. Notice that solutions of Riemann problems are not unique if the configuration resembles Fig. 6(b): both U_M and U_T serve as middle states in solutions of the Riemann problem with data U_L and U_R.

In the following, we present a detailed picture of the behavior of integral curves near the boundary of an elliptic region. We employ the approach of Palmeira [28], who studied integral curves for quadratic models with compact elliptic regions. One consequence of this analysis is that the configuration of Fig. 6(a) is generic, whereas points such as T in Figs. 6(b) and 6(d) are isolated points for generic flux functions. Thus the situation of Fig. 6(b), in which solutions of Riemann problems are not unique, does not occur generically. We emphasize that the present results are not restricted to quadratic models: the flux functions need satisfy only smoothness and genericity assumptions.

A rarefaction wave of a given family i is constructed using a curve in state space such

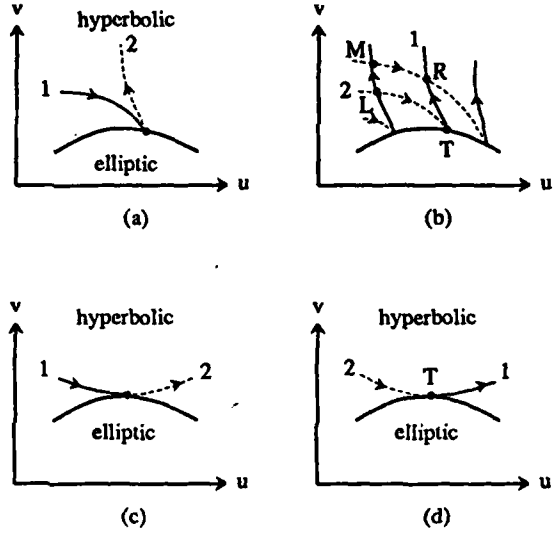

Fig. 6: Rarefaction curves near an elliptic region. In (a) and (c), there are no transitional rarefaction waves; in (b) and (d), the curves through points such as T correspond to transitional rarefaction waves. For generic fluxes, points such as T are isolated, so that configuration (b), which causes nonuniqueness, does not arise.

that its tangent $\dot{U}$ is a right eigenvector:

$$F'(U)\dot{U} = \lambda_i(U)\dot{U} \ . \tag{4.1}$$

In the neighborhood of a point of strict hyperbolicity, where the eigenvalues are real and distinct, such a curve is constructed by choosing a smooth field r_i of right eigenvectors and integrating the differential equation

$$\dot{U} = r_i(U) \ . \tag{4.2}$$

This choice is not generally possible, however, near a point where eigenvalues coincide.

To address this problem, we adopt a global geometric approach. Notice that the matrix $F'(U) - \lambda_i(U)$ has rank $n-1$ in the strictly hyperbolic region, so that Eq. (4.1) constrains $\dot{U}$ to lie in a line. From this perspective, we can construct rarefaction waves using integral curves of line fields. There are n distinct line fields defined throughout the strictly hyperbolic region. As we explain below, however, two of these line fields join smoothly at the boundary of this region, where eigenvalues coincide. In fact, when $n = 2$, the line fields may be regarded as projections of a single line field that is defined on a larger space.

Remark: A line field in an n-dimensional manifold can be specified by intersecting $n-1$ fields of tangent hyperplanes, so long as they are linearly independent. It proves convenient to regard any $n-1$ fields of tangent hyperplanes as defining a line field; in this case, points where the hyperplanes are not independent are called *critical points* of the line field.

Let us now restrict to the case of two conservation laws. Recall that lines through the origin in $\mathbf{R}^2$ form the one-dimensional real projective space RP^1. A point in RP^1 may be identified with a normalized vector $\pm(\cos\varphi, \sin\varphi)^{\mathrm{T}}$, modulo sign; as a coordinate for RP^1, therefore, we take $\varphi \in (-\pi/2, \pi/2]$ to correspond to the line through the origin that lies at angle φ. In these terms, a line field on $\mathbf{R}^2$ associates a point in RP^1 to each point in $\mathbf{R}^2$.

Following Palmeira, we introduce the space $\mathcal{P} = \mathbf{R}^2 \times RP^1$ of lines through points $U = (u, v)^{\mathrm{T}} \in \mathbf{R}^2$. The map $(U, \varphi) \mapsto U$ projects $\mathcal{P}$ onto $\mathbf{R}^2$, making $\mathcal{P}$ into a fiber bundle. A line field on $\mathbf{R}^2$ may be regarded as associating a point $(U, \varphi(U)) \in \mathcal{P}$ to each point $U \in \mathbf{R}^2$. An integral curve $\xi \mapsto U(\xi)$ of such a line field is the projection of the curve defined by $\xi \mapsto (U(\xi), \varphi(U(\xi))$; this curve in $\mathcal{P}$ is called the lift of the curve in $\mathbf{R}^2$. By definition, $\dot{U}$ lies at angle φ, so that $-\sin\varphi\,\dot{u} + \cos\varphi\,\dot{v} = 0$. This means that the vector $(\dot{U}, \dot{\varphi})$ is constrained to lie in the plane defined by the differential expression

$$-\sin\varphi\,du + \cos\varphi\,dv = 0\,. \tag{4.3}$$

In other words, the tangent vector of the lifted curve lies in the tangent plane at (U, φ) given by Eq. (4.3).

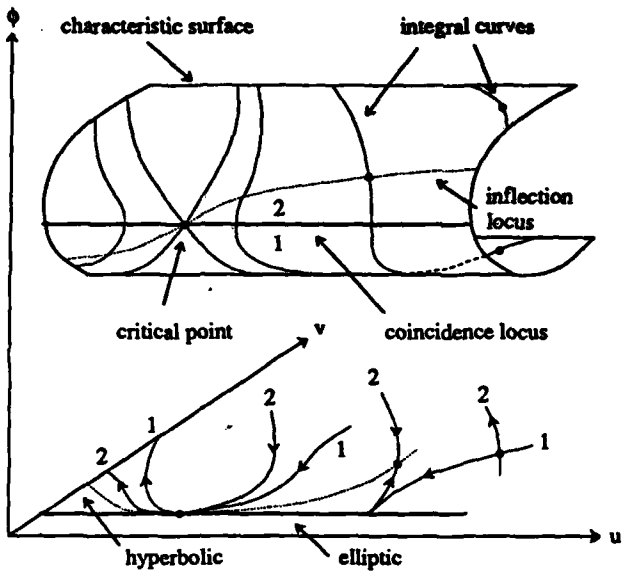

Fig. 7: A portion of the characteristic surface in the space $\mathcal{P}$. The surface folds along the coincidence locus, which projects onto the boundary of the elliptic region. Typical integral curves are drawn on the surface; their projections onto the u-v plane are rarefaction curves.

The line fields of interest to us are associated with eigenvectors of the Jacobian derivative matrix for the system of conservation laws. Let (U, φ) be a point in $\mathcal{P}$; then $(\cos\varphi, \sin\varphi)^{\mathrm{T}}$ is a right eigenvector of $F'(U)$ if and only if

$$\mathcal{F}(U,\varphi) = (-\sin\varphi, \cos\varphi)F'(U)\begin{pmatrix}\cos\varphi\\ \sin\varphi\end{pmatrix} \tag{4.4}$$

is zero. Thus we are led to study the surface $\mathcal{F} = 0$ in $\mathcal{P}$; we call it the *characteristic surface* for the system of conservation laws. The plane tangent to $\mathcal{P}$ defined by Eq. (4.3), when intersected with the plane tangent to the characteristic surface, defines a line field on this surface. The integral curves of this line field project onto solutions of Eq. (4.1), by virtue of Eq. (4.3). A portion of a characteristic surface is depicted in Fig. 7.

Recall that (U,φ) is a *regular point* of $\mathcal{F}$ if $(\mathcal{F}_u, \mathcal{F}_v, \mathcal{F}_\varphi) \neq (0,0,0)$ at (U,φ), and that v is a *regular value* of $\mathcal{F}$ if all points (U,φ) for which $\mathcal{F}(U,\varphi) = v$ are regular. The characteristic surface is a smooth, two-dimensional manifold in a neighborhood of a regular point, so that the whole characteristic surface is a smooth manifold provided that $v = 0$ is a regular value. Sard's theorem implies that regular values are generic if the flux F is smooth, but in general the characteristic surface might have singularities and self-intersections. The global structure of the characteristic surface is described for some examples in App. B.

In working with general conservation laws, it is convenient to represent the 2×2 matrix $F'(U)$ as

$$F'(U) = \begin{pmatrix} d+a & b+c \\ b-c & d-a \end{pmatrix} , \tag{4.5}$$

in terms of the functions a, b, c, and d of U (*cf.* Ref. [31]). Thus

$$\mathcal{F} = b\cos 2\varphi - a\sin 2\varphi - c \, . \tag{4.6}$$

Furthermore, in analogy with Eq. (4.4), we define the function λ on $\mathcal{P}$ by

$$\begin{aligned} \lambda(U,\varphi) &= (\cos\varphi, \sin\varphi) F'(U) \begin{pmatrix} \cos\varphi \\ \sin\varphi \end{pmatrix} \\ &= a\cos 2\varphi + b\sin 2\varphi + d \, . \end{aligned} \tag{4.7}$$

As seen from Eqs. (4.4) and (4.7), if a point (U,φ) lies on the characteristic surface $\mathcal{F} = 0$, then $\lambda(U,\varphi)$ is the eigenvalue of $F'(U)$ for the right eigenvector $(\cos\varphi, \sin\varphi)^{\mathrm{T}}$. Moreover, the following relations are easily verified:

$$(\lambda - d)^2 + (\mathcal{F} + c)^2 = a^2 + b^2 \; ; \tag{4.8}$$

$$-\tfrac{1}{2}\mathcal{F}_\varphi = \lambda - d \; ; \tag{4.9}$$

$$-\tfrac{1}{4}\mathcal{F}_{\varphi\varphi} = \mathcal{F} + c = \tfrac{1}{2}\lambda_\varphi \, . \tag{4.10}$$

We define the *coincidence locus* to comprise points (U,φ) on the characteristic surface at which $\lambda_1(U) = \lambda_2(U)$. (See Fig. 7.) The next result characterizes this locus.

Proposition 4.1: *The coincidence locus comprises points satisfying* $\mathcal{F} = 0$ *and* $\mathcal{F}_\varphi = 0$. *The following are equivalent at a coincidence point, provided that it is a regular point of* $\mathcal{F}$: *(i) the projection of the characteristic surface is a fold; (ii)* $\lambda_\varphi \neq 0$; *(iii)* $c \neq 0$; *and (iv)* $(a, b) \neq (0, 0)$.

Proof: The characteristic speeds coincide if and only if the discriminant $\mathrm{discrm}\, F'(U) = 4(a^2 + b^2 - c^2)$ vanishes. According to Eq. (4.8), $a^2 + b^2 - c^2 = (\lambda - d)^2$ on the surface $\mathcal{F} = 0$, so that by Eq. (4.9), coincidence occurs precisely when $\mathcal{F}_\varphi = 0$.

In particular, the projection $(U, \varphi) \mapsto U$, restricted to the characteristic surface, is singular at a coincidence point. This singularity is of fold type when $\mathcal{F}_{\varphi\varphi} \neq 0$. By Eqs. (4.10) with $\mathcal{F} = 0$, conditions (i)–(iii) are equivalent, and because $a^2 + b^2 = c^2$ at a coincidence point, conditions (iii) and (iv) are equivalent. □

Accordingly, the coincidence locus is a smooth curve through those coincidence points for which the matrix

$$\begin{pmatrix} \mathcal{F}_u & \mathcal{F}_v & 0 \\ \mathcal{F}_{\varphi u} & \mathcal{F}_{\varphi v} & \mathcal{F}_{\varphi\varphi} \end{pmatrix} \tag{4.11}$$

has rank two. A sufficient condition is that the coincidence point be a regular fold point. Vectors tangent to the coincidence locus belong to the kernel of this matrix. Notice that a tangent vector at a regular fold point cannot be vertical (*i.e.*, have vanishing u and v components).

Corresponding to the integral curves in $\mathbf{R}^2$ used to construct rarefaction waves are lifted curves lying in $\mathcal{P}$. In addition to satisfying Eq. (4.3), these lifted curves belong to the characteristic surface $\mathcal{F} = 0$, so that $d\mathcal{F} = 0$ along them. Therefore we consider integral curves of the line field in $\mathcal{P}$ given by

$$\mathcal{F}_u\, du + \mathcal{F}_v\, dv + \mathcal{F}_\varphi\, d\varphi = 0\ , \tag{4.12}$$

$$-\sin\varphi\, du + \cos\varphi\, dv = 0\ . \tag{4.13}$$

If such an integral curve starts at a point in the characteristic surface, then it lies entirely within the characteristic surface, as shown in Fig. 7.

Integral curves of Eqs. (4.12) and (4.13) can be obtained locally by integrating the differential equations

$$\dot{u} = -\mathcal{F}_\varphi \cos\varphi\ , \tag{4.14}$$

$$\dot{v} = -\mathcal{F}_\varphi \sin\varphi \,, \tag{4.15}$$

$$\dot{\varphi} = \mathcal{F}_u \cos\varphi + \mathcal{F}_v \sin\varphi \,. \tag{4.16}$$

Indeed, this local vector field satisfies Eqs. (4.12) and (4.13), and it vanishes when these two equations are linearly dependent. (Notice, however, that Eqs. (4.14)–(4.16) do not define a global vector field on $\mathcal{P}$: they are not invariant under the map $\varphi \mapsto \varphi + \pi$.) Thus critical points of the line field occur precisely when $\mathcal{F}_\varphi = 0$ and

$$\mathcal{F}_u \cos\varphi + \mathcal{F}_v \sin\varphi = 0 \,. \tag{4.17}$$

We say that a point on the coincidence locus is *critical* whenever Eq. (4.17) holds. Such points play a significant role in determining the structure of integral curves on the characteristic surface [28]. We emphasize, however, that for generic choices of the flux functions in the conservation laws, critical points will be isolated points on the coincidence locus (*cf.* App. B.2). At generic points on the coincidence locus, $\dot{u} = 0$, $\dot{v} = 0$, and $\dot{\varphi} \neq 0$; therefore the integral curve is vertical, and the projected integral curve has a cusp (see Fig. 7).

Also of importance is the *family* to which a point on the characteristic surface belongs. Noting that coincidence of eigenvalues occurs when $\lambda = d$, we define the 1-family region $\mathcal{P}_1$ in $\mathcal{P}$ to comprise points for which $\lambda < d$; similarly, $\lambda > d$ in the 2-family region $\mathcal{P}_2$. This definition is appropriate because of the following consideration. Suppose that (U, φ_1) and (U, φ_2) are two points in the characteristic surface that project onto the same point U; suppose further that $(U, \varphi_1) \in \mathcal{P}_1$ and $(U, \varphi_2) \in \mathcal{P}_2$. Then $\lambda(U, \varphi_1) < d(U) < \lambda(U, \varphi_2)$. Consequently, $\lambda(U, \varphi_1) = \lambda_1(U)$ and $\lambda(U, \varphi_2) = \lambda_2(U)$, while $(\cos\varphi_1, \sin\varphi_1)^{\mathrm{T}}$ and $(\cos\varphi_2, \sin\varphi_2)^{\mathrm{T}}$ are the corresponding right eigenvectors. If the system of conservation laws is strictly hyperbolic, then the characteristic surface consists of two distinct sheets, belonging to the regions $\mathcal{P}_1$ and $\mathcal{P}_2$. More generally, these sheets join along the coincidence locus, as in Fig. 7.

With this notion of family, we can state the main result of this section.

Theorem 4.2: *Consider a regular fold point on the coincidence locus, and suppose that it is not critical. Then the integral curve through this point crosses the coincidence locus*

transversally, and its projection, a rarefaction curve, has a cusp. Moreover, if the integral curve is followed in the direction of increasing eigenvalue, then it leads from the 1-family region to the 2-family region.

Proof: According to Eqs. (4.14)–(4.16), the integral curve is vertical at such a point: $\dot{u} = 0$, $\dot{v} = 0$, and $\dot{\varphi} \neq 0$. Therefore the integral curve is transverse to the coincidence locus, whose tangent is not vertical. Also, the integral curve leads from $\mathcal{P}_1$ to $\mathcal{P}_2$ because the derivative of $\lambda - d$ along the curve is $\lambda_\varphi \dot{\varphi} \neq 0$. □

Transitional rarefaction waves arise only when an integral curve leads from the 2-family region into the 1-family region when traversed with increasing eigenvalue. By Theorem 4.2 this is possible only for integral curves through special points on the coincidence locus: critical points, where Eq. (4.17) holds; non-fold points, where $\mathcal{F}_{\varphi\varphi} = 0$ (which usually correspond to cusps in the coincidence locus, as projected onto state space); and irregular points, where $(\mathcal{F}_u, \mathcal{F}_v) = (0, 0)$ (at which the characteristic surface need not be a manifold). Such singular points, being characterized by extra functional conditions, generically are isolated points on the coincidence locus.

Corollary 4.3: *For generic choices of the flux functions that define the system of conservation laws, transitional rarefaction waves arise only from integral curves through isolated points on the coincidence locus.*

Rarefaction waves correspond to segments of integral curves along which the characteristic speed does not decrease. To reflect this, the integral curves shown in Fig. 7 have been oriented according to the variation of λ. The orientation changes at points where $\lambda_i'(U) r_i(U) = 0$, which are called inflection points by analogy with scalar conservation laws. In the present geometric framework, the *inflection locus* is defined to be points on the characteristic surface for which $d\lambda = 0$ in the direction of the integral curve, *i.e.*,

$$\det \begin{pmatrix} \mathcal{F}_u & \mathcal{F}_v & \mathcal{F}_\varphi \\ -\sin\varphi & \cos\varphi & 0 \\ \lambda_u & \lambda_v & \lambda_\varphi \end{pmatrix} = 0 \,. \tag{4.18}$$

The following result helps elucidate the behavior of integral curves near critical points.

Proposition 4.4: *A regular fold point on the coincidence locus is a point of inflection if and only if it is a critical point.*

Proof: When $\mathcal{F}_\varphi = 0$, Eq. (4.18) becomes $\lambda_\varphi [\mathcal{F}_u \cos\varphi + \mathcal{F}_v \sin\varphi] = 0$. □

As illustrated in Fig. 7, the inflection locus passing through the critical point permits a transitional rarefaction to occur even though neighboring integral curves lead from family 1 to family 2.

The constructions of this section have been applied by Palmeira to quadratic conservation laws [28]. (See the App. B.1 for another presentation of these computations.) Furthermore, Palmeira shows that the results obtained for quadratic models are stable under perturbations of the flux functions (in the C^3 Whitney topology). This is a first step in proving stability of solutions of Riemann problems with respect to changes in the conservation laws.

5. The Role of Transitional Waves in Solving Riemann Problems

A solution of a Riemann problem consists of a sequence of rarefaction waves and discontinuities. For various systems (*e.g.*, Refs. [35, 13, 9, 10, 14, 34]), the general Riemann problem cannot be solved globally if only Lax shock waves with viscous profiles are used: for certain left states, there are regions of right states for which there is no solution. In this section, we explain how transitional waves can be used to overcome this difficulty. The transitional shock waves define a certain map in state space; for simplicity, we describe this map for systems of two conservation laws, although a straightforward generalization can be made to systems of arbitrary size. We begin by recalling the classical method for constructing local solutions of Riemann problems [25, 26].

The *1-wave curve* based upon a state U_0 consists of those states to which U_0 can be joined by a succession of 1-waves; a similar definition holds for 2-waves. Near U_0, each wave curve consists of a shock branch joined to a rarefaction branch (if U_0 is not on the inflection locus); an eigenvector of $F'(U_0)$ is tangent to these branches at U_0. To solve the Riemann problem near a left state U_L, the standard construction is to build the 1-wave curve based upon U_L, and then to build the 2-wave curve based upon each middle state U_M on the 1-wave curve. This is illustrated in Fig. 8 in the vicinity of U_L. (In Figs. 8 and 9, 1-wave curves are thicker than 2-wave curves, with solid curves being rarefaction curves and dashed curves being shock curves.) In this way, all neighboring states U_R are joined

to U_L by a 1-wave followed by a 2-wave. To carry out this procedure globally, detached branches of the wave curves must also be used. For example, a state U_R in the upper left corner of Fig. 8 is reached by a nonlocal 1-shock wave, U_M being a point on the Hugoniot branch above point C, followed by a 2-wave. As mentioned above, however, there might be right states that are not reached in this manner, such as points in the strip bounded by the 2-wave curves through B and C. To complete the solution, transitional waves are employed.

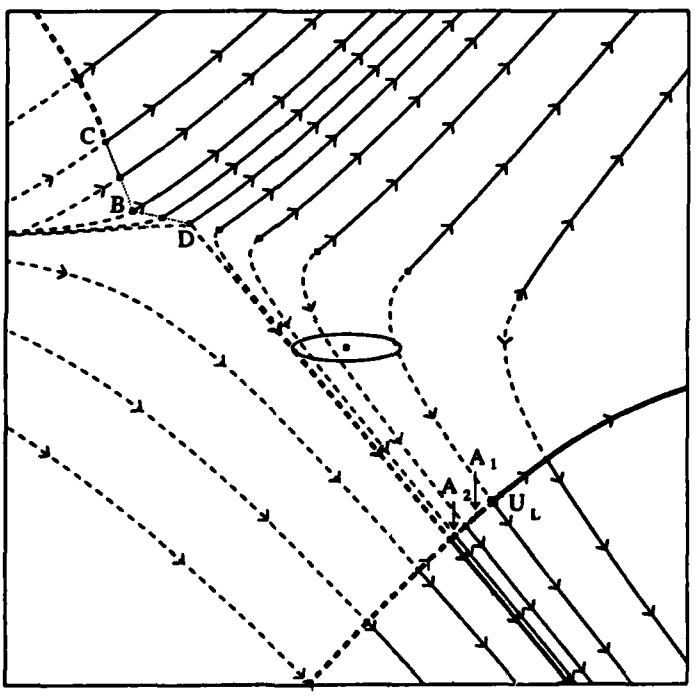

Fig. 8: Solutions of Riemann problems for a particular left state U_L. The system is a quadratic model with an elliptic region; all shock waves admit viscous profiles for a viscosity matrix D that differs from the identity. Points between B and C correspond to transitional shock waves from points between A_2 and A_1. Points between B and D correspond to nonlocal 2-shock waves from U_L, while points above C are nonlocal 1-shock waves.

First we describe the use of transitional shock waves. Based on part (a) of Theorem 3.5

for quadratic models, the class of transitional shock waves for generic flux functions is characterized by a *transitional map* X defined on an open set T, the transitional region. The transitional map carries each point U in T to a unique point $U' = X(U)$ in $T' = X[T]$ such that U and U' are connected by an admissible crossing discontinuity. We contrast this picture with that of Lax waves, where to each state there corresponds a curve of states. More generally, there might be several transitional maps. (For quadratic models, different maps are associated with different viscosity angles.)

Remark: We expect this map to be stable under small perturbations of the flux functions and of the viscosity matrix. Techniques such as those used in Ref. [36] should suffice to establish stability. This property is crucial to insure that these new shock waves have physical significance.

Transitional shock waves are used to solve Riemann problems in the following manner. For a given left state U_L, the 1-wave curve based on U_L is built. If the curve passes through the region T, then each state U_M on the curve in this region is joined to its image state $U'_M = X(U_M)$ by a transitional shock wave. Of course, the speed of this wave must exceed the speed of the 1-wave from U_L to U_M. Under this restriction, an image curve in the region T' is generated. Finally, 2-wave curves are drawn from points on this transitional curve, thus covering a region in state space. This construction is shown in Fig. 8 (the transitional regions are the same as in Fig. 5): the 1-wave curve passes through region T_1, and the portion $(A_1 A_2)$ is mapped onto the curve (CB). Therefore the strip left uncovered by Lax waves is filled by solutions composed of three wave groups, a 1-wave, a transitional shock wave, and a 2-wave. The procedure just outlined can be generalized to systems of arbitrary size.

Notice that because the transitional wave from A_1 to C has the same speed as the 1-shock wave from L to A_1, the points L, A_1, and C are all critical points of the dynamical system (2.10). This system has a saddle-saddle connection between A_1 and C, so that it is subject to bifurcation. Indeed, points on the branch of 1-shock waves above C are joined to U_L by a node-saddle connecting orbit, whereas points on the continuation of this branch below C are not, even though they correspond to Lax waves. Similarly, the transitional

wave from A_2 to B is an endpoint of the transitional curve because the critical point B is not hyperbolic. The curve joining points B and D is reached by (admissible) nonlocal 2-shock waves.

The picture just described is different from that obtained in the nongeneric case of Theorem 3.5: in part (b), the transitional region is not open, being open rays of the viscosity lines, and the corresponding transitional shock waves comprise open segments on these lines. This situation arises in several examples in which transitional waves are used [35, 9, 10, 34] because D is taken to be the identity matrix. Parameter and equation counting for saddle-saddle connecting orbits are inconsistent with this picture [30]. This nongeneric case is illustrated in Fig. 9, which depicts the limits of solutions in Fig. 8 as D approaches the identity matrix: the curve (A_1A_2) collapses to a single point A, which is the left state for transitional shock waves to points along (CB).

Figure 9 represents part of the solution for a symmetric quadratic model in Case II [21]; this solution enforces the viscous profile admissibility criterion. In Refs. [21, 32], solutions for Case II quadratic models are obtained using all shock waves obeying Lax's characteristic inequalities, regardless of whether these shock waves possess viscous profiles. In fact, nonlocal 1- and 2-shock waves that do not have viscous profiles appear in these solutions, such as nonlocal 1-shock waves on the Hugoniot branch below point C and nonlocal 2-shock waves to points near (CB) in Fig. 8. This is an instructive example in which two distinct solutions of the general Riemann problem arise from different choices of an admissibility criterion. Each of these choices yields a solution that is complete and unique.

Remark: We expect that standard numerical methods employed in solving the Cauchy problem for conservation laws are inaccurate if the solution involves transitional or nonlocal shock waves. The reasons are as follows. First, many numerical schemes spread a strong shock wave across several mesh zones, replacing it with many weak shock waves, each approximated by the local rarefaction curve; but this approximation is not valid for nonlocal shock waves, which are non-contractable. (Methods such as the random choice method [8] do not make this approximation.) Second, transitional shock waves are sensitive to the precise form of the diffusion term (cf. Figs. 8 and 9). In contrast to Lax shock waves, which are affected only by the overall magnitude of the viscosity, the asymptotic states in

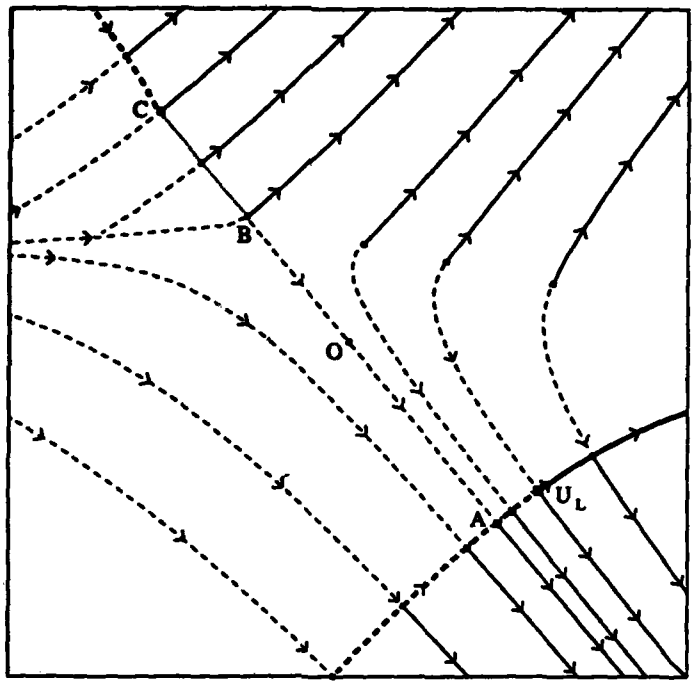

Fig. 9: Solutions of Riemann problems for a homogeneous quadratic model in Case II and a particular left state U_L. All shock waves admit viscous profiles for $D = I$. Points between B and C correspond to transitional shock waves from point A.

a crossing shock wave are dependent on the relative sizes of components of the viscosity matrix. Dissipative numerical schemes on coarse grids calculate transitional shock waves that correspond to the numerical viscosity, rather than the physical viscosity.

The usage of transitional rarefaction waves in solving Riemann problems is simpler; it resembles the degenerate case for transitional shock waves. As shown in §4, transitional rarefaction curves emanate from isolated points on the coincidence locus. For instance, in Case II quadratic models there is a single transitional rarefaction curve; in Fig. 8 it passes tangent to the top of the elliptic boundary, with the 2-family portion extending to the left, and the 1-family portion extending to the right. Suppose that the 1-wave curve through U_L intersects the 2-family portion of the transitional curve at U_M; then the 1-wave from

U_L to U_M can be followed by a transitional rarefaction wave from U_M to a point $U_{M'}$ on the 1-family portion, which in turn can be followed by a 2-wave. This construction is completely analogous to that used in specific examples [21, 32].

In summary, a transitional wave can appear between a 1-wave group and a 2-wave group in a solution of a Riemann problem. The procedure for constructing such solutions is to associate a transitional wave curve to the left state U_L. This transitional curve is obtained by applying the transitional map to the 1-wave curve in the case of shock waves, and by following an integral curve in the case of rarefaction waves. More generally, composite waves containing transitional waves along with Lax waves can occur [17, 14]; see Figs. 2(c) and (d).

6. Summary

Transitional waves, which are not associated with a particular characteristic family, arise in non–strictly-hyperbolic systems of conservation laws. Because of such waves, the solution of a Riemann problem for a system of n conservation laws might contain more than n wave groups.

Transitional shock waves are discontinuous solutions that possess viscous profiles corresponding to saddle-saddle connecting orbits. For transitional shock waves, the association of U_L with U_R is a map defined on a region in state space (for generic viscosity matrices); this has been demonstrated explicitly for conservation laws with quadratic flux functions, where saddle-saddle connecting orbits are straight line segments.

Transitional rarefaction waves are continuous solutions that switch from a faster family to a slower one. Using a geometric framework, the generic nature of rarefaction waves near an elliptic region in systems of two conservation laws has been established: if a rarefaction curve intersects the elliptic boundary, then except at isolated points it switches from a slower family to a faster one and forms a cusp; the exceptional points are where the rarefaction curve is transitional and passes tangent to the elliptic region.

Transitional waves play a significant role in solving the Riemann problem for non–strictly-hyperbolic systems. This is illustrated in a quadratic model for which the general Riemann problem has two distinct solutions, both complete and unique, depending on the

admissibility criterion imposed on shock waves. One solution uses all waves satisfying the characteristic criterion, some of which do not possess viscous profiles; the other uses the viscous profile criterion and requires transitional shock waves.

Acknowledgments

We thank Prof. Mark Ashbaugh for bringing the work of Chicone to our attention. We are grateful also to Prof. Geovan Tavares dos Santos and Dr. M. Elasir Gomes for discussions concerning Theorem 3.8, and to Prof. C. Frederico Palmeira for conversations about transitional rarefaction waves.

The hospitality of the Courant Institute of Mathematical Sciences of New York University, the Departments of Mathematics at Pontifícia Universidade Católica of Rio de Janeiro and at the University of Wyoming, the Department of Computer Sciences and the Mathematics Research Center at the University of Wisconsin–Madison, and the Instituto de Matemática Pura e Aplicada is gratefully acknowledged.

Appendix A. Proof of Corollary 3.9

In this appendix, we give a proof of Corollary 3.9 using Gomes' Theorem 3.8. Consider a quadratic dynamical system in the plane

$$\dot{u} = P(u,v)\ , \tag{A.1}$$

$$\dot{v} = Q(u,v)\ , \tag{A.2}$$

where P and Q are quadratic polynomials in u and v and the dot denotes differentiation with respect to the independent variable ξ. The behavior of solutions is affected not only by critical points (u_c, v_c) in the finite plane, where $P(u_c, v_c) = 0$ and $Q(u_c, v_c) = 0$, but also by the behavior of P and Q near infinity, *i.e.*, the asymptotic directions of the vector field.

To study the behavior near infinity, we make a (singular) change of independent variables from ξ to η by setting $d/d\eta = R^{-1} d/d\xi$, where $R = (u^2 + v^2)^{\frac{1}{2}}$. This allows us to exploit the approximate homogeneity of P and Q for large R:

$$P(u,v) = R^2\Big\{P_2(u/R, v/R) + O(R^{-1})\Big\}\ , \tag{A.3}$$

$$Q(u,v) = R^2\Big\{Q_2(u/R, v/R) + O(R^{-1})\Big\}\ , \tag{A.4}$$

P_2 and Q_2 being the homogeneous quadratic parts of P and Q, respectively. Introducing polar coordinates, $u = R\cos\varphi$ and $v = R\sin\varphi$, and denoting $\rho = R^{-1}$, a straightforward calculation shows that

$$\varphi' = \cos\varphi\, Q_2(\cos\varphi, \sin\varphi) - \sin\varphi\, P_2(\cos\varphi, \sin\varphi) + O(\rho)\ , \tag{A.5}$$

$$\rho' = -\rho\Big\{\cos\varphi\, P_2(\cos\varphi, \sin\varphi) + \sin\varphi\, Q_2(\cos\varphi, \sin\varphi) + O(\rho)\Big\}\ , \tag{A.6}$$

where the prime denotes differentiation with respect to η. Therefore a *critical point at infinity* occurs if and only if $\rho = 0$ and

$$\cos\varphi\, Q_2(\cos\varphi, \sin\dot{\varphi}) - \sin\varphi\, P_2(\cos\varphi, \sin\varphi) = 0\ . \tag{A.7}$$

Eq. (A.7) is a homogeneous cubic polynomial in $\sin\varphi$ and $\cos\varphi$; its roots give the asymptotic directions of the vector field. The eigenvalues of the linearization of Eqs. (A.5) and (A.6) near a critical point at infinity are

$$\mu_\varphi = \frac{d}{d\varphi}\Big\{\cos\varphi\, Q_2(\cos\varphi, \sin\varphi) - \sin\varphi\, P_2(\cos\varphi, \sin\varphi)\Big\} \tag{A.8}$$

and

$$\mu_\rho = -\Big\{\cos\varphi\, P_2(\cos\varphi, \sin\varphi) + \sin\varphi\, Q_2(\cos\varphi, \sin\varphi)\Big\}\ , \tag{A.9}$$

corresponding to the φ and ρ directions.

For the dynamical system

$$D\,\dot{U}(\xi) = -s\,[U(\xi) - U_-] + F(U(\xi)) - F(U_-) \tag{A.10}$$

derived from a quadratic system of conservation laws, $(P_2, Q_2)^{\mathrm{T}} = D^{-1}F_2$, where F_2 is the homogeneous quadratic part of the flux F. Let α_D, β_D, $\tilde{\alpha}_D$, and $\tilde{\beta}_D$ denote the functions associated with $D^{-1}F$ that are defined (for F) in Eqs. (3.7), (3.8), (3.10), and (3.11). In these terms, a critical point at infinity occurs precisely when $\rho = 0$ and

$$\alpha_D(\varphi)\cos\varphi + \beta_D(\varphi)\sin\varphi = 0\ , \tag{A.11}$$

and the eigenvalues at such a point are

$$\mu_\varphi = \tfrac{1}{2}\frac{d}{d\varphi}\Big\{\alpha_D(\varphi)\cos\varphi + \beta_D(\varphi)\sin\varphi\Big\} \tag{A.12}$$

and

$$\mu_\rho = -\tfrac{1}{2}\left\{\tilde{\alpha}_D(\varphi)\cos\varphi + \tilde{\beta}_D(\varphi)\sin\varphi\right\} . \qquad (A.13)$$

By definition, an angle φ satisfying Eq. (A.11) is a viscosity angle; thus critical points at infinity occur at viscosity angles. Notice that solutions of Eq. (A.11) come in pairs, φ and $\varphi + \pi$, corresponding to antipodal critical points at infinity. Consequently, we have demonstrated the following.

Lemma A.1: *Suppose that a quadratic model has more than one viscosity line. Then there are more than two critical points at infinity for the dynamical system (A.10).*

We remark that Eq. (A.11) is a homogeneous cubic polynomial in $\cos\varphi$ and $\sin\varphi$, and if the roots of this cubic are simple, then $\mu_\varphi \neq 0$. Also, $\mu_\rho \neq 0$ if and only if the viscosity angle φ is not exceptional.

Lemma A.1 verifies the hypothesis of Theorem 3.8 concerning critical points at infinity; the next lemma verifies the hypothesis about critical points in the finite plane.

Lemma A.2: *Suppose that the flux for a quadratic model is a gradient. Then if the viscosity matrix D is symmetric and positive definite, the critical points in the finite plane for the dynamical system (A.10) have real eigenvalues.*

Proof: The linearization of Eq. (A.10) near a critical point U_c is

$$D\dot{U} = [-s + F'(U_c)](U - U_c) , \qquad (A.14)$$

so that the eigenvalues of the linearization are eigenvalues of the matrix $D^{-1}[-s + F'(U_c)]$. If D is symmetric and positive definite, then this matrix is similar to, and therefore has the same eigenvalues as, the matrix $D^{-\frac{1}{2}}[-s + F'(U_c)]D^{-\frac{1}{2}}$. When F is a gradient, say $F = C'$, the Jacobian derivative $F' = C''$ is symmetric. Consequently, the latter matrix, being symmetric, has real eigenvalues. □

Combining these two results with Theorem 3.8 proves Corollary 3.9.

Appendix B. Examples of Characteristic Surfaces

In this appendix, we present two examples of the constructions of §4 for rarefaction waves.

B.1 Quadratic Models

The approach of §4 was developed by Palmeira [28] for quadratic models with compact elliptic regions; the results carry over to general quadratic models. Using the notation of §3a, it is simple to verify that

$$\mathcal{F}(u,v,\varphi) = \alpha(\varphi)u + \beta(\varphi)v + \gamma(\varphi) \tag{B.1}$$

and

$$\lambda(u,v,\varphi) = \tilde{\alpha}(\varphi)u + \tilde{\beta}(\varphi)v + \tilde{\gamma}(\varphi)\ . \tag{B.2}$$

Thus the characteristic surface $\mathcal{F} = 0$ is ruled: each horizontal plane $\varphi =$ const. intersects the surface in a straight line $\alpha(\varphi)u + \beta(\varphi)v + \gamma(\varphi) = 0$, the projection of which is a characteristic line. The surface is regular except when $\alpha(\varphi) = \beta(\varphi) = \gamma(\varphi) = 0$ and $\mathcal{F}_\varphi = 0$ [see Eq. (B.4) below].

The coincidence locus is defined by the equations $\mathcal{F} = 0$ and $\mathcal{F}_\varphi = 0$, *i.e.*,

$$\alpha(\varphi)u + \beta(\varphi)v + \gamma(\varphi) = 0\ , \tag{B.3}$$

$$\alpha'(\varphi)u + \beta'(\varphi)v + \gamma'(\varphi) = 0\ . \tag{B.4}$$

Notice that these are also the equations for the envelope of the characteristic lines. For simplicity, we assume that the determinant $\mathcal{D} = \alpha\,\beta' - \beta\,\alpha'$ does not vanish identically. Then the linear equations (B.3) and (B.4) may be solved to express u and v on the coincidence locus in terms of φ: $u = u_c(\varphi)$ and $v = v_c(\varphi)$, where

$$u_c = -\left[\gamma\,\beta' - \beta\,\gamma'\right]/\mathcal{D}\ , \tag{B.5}$$

$$v_c = -\left[\alpha\,\gamma' - \gamma\,\alpha'\right]/\mathcal{D}\ . \tag{B.6}$$

Despite appearances, $\mathcal{D}$ and the numerators of u_c and v_c are linear, not quadratic, in $\sin 2\varphi$ and $\cos 2\varphi$. Thus the coincidence locus is a conic section; any asymptotes occur at the angles φ where $\mathcal{D}(\varphi) = 0$.

A coincidence point is a fold point unless $\mathcal{F}_{\varphi\varphi} = 0$. Evaluated on the surface $\mathcal{F} = 0$,

$$\tfrac{1}{4}\mathcal{F}_{\varphi\varphi}(u,v,\varphi) = \alpha_0 u + \beta_0 v + \gamma_0\ ,$$

where $\alpha_0 = \frac{1}{2}(a_2 - b_1)$, $\beta_0 = \frac{1}{2}(b_2 - c_1)$, and $\gamma_0 = \frac{1}{2}(d_2 - e_1)$ are the φ-independent parts of α, β, and γ. Therefore a coincidence point is a fold point so long as $\alpha_0 u_c(\varphi) + \beta_0 v_c(\varphi) + \gamma_0 \neq 0$. A simplification occurs here also: $\alpha_0 u_c + \beta_0 v_c + \gamma_0 = -\frac{1}{4}\eta/\mathcal{D}$ with η constant. Provided that $\eta \neq 0$, all points on the coincidence locus are fold points.

In terms of the parameterization of the coincidence locus, any solution (u, v) of $\mathcal{F}(u, v, \varphi) = 0$ takes the form

$$u = u_c(\varphi) - \beta(\varphi) \cdot \kappa \,, \tag{B.7}$$

$$v = v_c(\varphi) + \alpha(\varphi) \cdot \kappa \tag{B.8}$$

for some $\kappa \in \mathbf{R}$ (except when $\mathcal{D}(\varphi) = 0$). Thus φ and κ give global coordinates for the characteristic surface, and $\kappa = 0$ defines the coincidence locus.

To determine the differential equations for integral curves in these coordinates, we require formulae for the derivatives u_c' and v_c'. Substituting u_c and v_c into Eqs. (B.3) and (B.4) and differentiating shows that

$$\alpha u_c' + \beta v_c' = 0 \,, \tag{B.9}$$

$$\alpha' u_c' + \beta' v_c' = -4\left[\alpha_0 u_c + \beta_0 v_c + \gamma_0\right] \tag{B.10}$$

Thus $u_c' = -\beta\,\eta/\mathcal{D}^2$ and $v_c' = \alpha\,\eta/\mathcal{D}^2$.

Expressed in global coordinates, the equation defining integral curves is

$$\begin{aligned} 0 &= -\sin\varphi\, du + \cos\varphi\, dv \\ &= \left[\alpha\cos\varphi + \beta\sin\varphi\right] d\kappa \\ &\quad + \left\{\left[\alpha\cos\varphi + \beta\sin\varphi\right]\eta/\mathcal{D}^2 + \left[\alpha'\cos\varphi + \beta'\sin\varphi\right]\cdot\kappa\right\} d\varphi \end{aligned} \tag{B.11}$$

Thus integral curves may be obtained (locally) by solving

$$\dot{\varphi} = -\left[\alpha\cos\varphi + \beta\sin\varphi\right] \,, \tag{B.12}$$

$$\dot{\kappa} = \left[\alpha\cos\varphi + \beta\sin\varphi\right]\eta/\mathcal{D}^2 + \left[\alpha'\cos\varphi + \beta'\sin\varphi\right]\cdot\kappa \,. \tag{B.13}$$

These equations yield a first-order, linear differential equation for κ as a function of φ. Critical points of the dynamical system (B.12) and (B.13) occur precisely when $\alpha\cos\varphi +$

$\beta \sin\varphi = 0$ and $\kappa = 0$, *i.e.*, at coincidence points for which φ is an asymptotic angle. In other words, the critical points occur where the bifurcation lines are tangent to the coincidence locus.

The inflection locus is defined by Eq. (4.18). To solve this equation in the present case, notice that $\lambda_\varphi = -\frac{1}{2}\mathcal{F}_{\varphi\varphi} = \frac{1}{2}[\eta/\mathcal{D} - \mathcal{D}' \cdot \kappa]$ and that $\mathcal{F}_\varphi = \mathcal{D} \cdot \kappa$. Then the inflection locus is determined by the equation

$$\left[\left(\tfrac{1}{2}\mathcal{D}'\alpha + \mathcal{D}\tilde{\alpha}\right)\cos\varphi + \left(\tfrac{1}{2}\mathcal{D}'\beta + \mathcal{D}\tilde{\beta}\right)\sin\varphi\right] \cdot \kappa = \tfrac{1}{2}\left[\alpha\cos\varphi + \beta\sin\varphi\right]\eta/\mathcal{D}\,. \qquad (B.14)$$

The quantities in parentheses in this equation simplify to linear expressions in $\sin 2\varphi$ and $\cos 2\varphi$.

B.2 Keyfitz-Kranzer Models

Systems of conservation laws of the form

$$u_t + [u\Phi(u,v)]_x = 0\,, \qquad (B.15)$$

$$v_t + [v\Phi(u,v)]_x = 0 \qquad (B.16)$$

have been studied as models for elastic strings [23, 24] and for multiphase flows in petroleum reservoirs [16, 37, 22, 27]. For such a system,

$$\mathcal{F}(u,v,\varphi) = [-u\sin\varphi + v\cos\varphi]\,[\Phi_u(u,v)\cos\varphi + \Phi_v(u,v)\sin\varphi] \qquad (B.17)$$

and

$$\lambda(u,v,\varphi) = \Phi(u,v) + [u\cos\varphi + v\sin\varphi]\,[\Phi_u(u,v)\cos\varphi + \Phi_v(u,v)\sin\varphi]\,. \qquad (B.18)$$

Therefore the characteristic surface is the intersection of two surfaces: the ruled surface where $\mathcal{F}_{\text{ruled}}(u,v,\varphi) = -u\sin\varphi + v\cos\varphi$ is zero; and the surface where $\mathcal{F}_{\text{contact}}(u,v,\varphi) = \Phi_u(u,v)\cos\varphi + \Phi_v(u,v)\sin\varphi$ is zero, which we call the "contact" surface because of its relation to the linearly degenerate wave mode.

For a point (u,v,φ) on the ruled surface, $u = \kappa\cos\varphi$ and $v = \kappa\sin\varphi$ for some $\kappa \in \mathbf{R}$, so that $\mathcal{F}_\varphi(u,v,\varphi) = -\kappa\mathcal{F}_{\text{contact}}(u,v,\varphi)$. In particular, $\lambda = \Phi + u\Phi_u + v\Phi_v$. Similarly,

for a point on the contact surface, $\Phi_u = -\mu \sin\varphi$ and $\Phi_v = \mu \cos\varphi$ for some $\mu \in \mathbf{R}$, $\mathcal{F}_\varphi(u,v,\varphi) = \mu \mathcal{F}_{\text{ruled}}(u,v,\varphi)$, and $\lambda = \Phi$.

It follows that the coincidence locus, where both $\mathcal{F}$ and $\mathcal{F}_\varphi$ vanish, comprises the intersection of the ruled and contact surfaces, together with the vertical line $u = 0$, $v = 0$. Necessarily, the characteristic surface fails to be regular at coincidence points, where it is not a manifold; indeed, $\mathcal{F}_u$ and $\mathcal{F}_v$, as well as $\mathcal{F}_\varphi$, vanish on the coincidence locus. The projection of this locus onto the u-v plane is given by the equation

$$u\Phi_u + v\Phi_v = 0 \,, \tag{B.19}$$

and it is bordered on both sides by regions of strict hyperbolicity, instead of separating a hyperbolic region from an elliptic region.

Remark: In one sense, the system of conservation laws (B.16) and (B.17) is not generic: the flux functions take a special form $f(u,v) = u\Phi(u,v)$ and $g(u,v) = v\Phi(u,v)$. This form is not stable under general perturbations, which would break the intersecting surfaces apart and remove the singularity. However, the conservation laws may be regarded as generic, in a different sense, provided that the physical system being modeled imposes this special form of the flux functions and allows for general perturbations of Φ.

Evaluated on the ruled surface, the equation defining integral curves is

$$0 = -\sin\varphi\, du + \cos\varphi\, dv = \kappa\, d\varphi \,. \tag{B.20}$$

Thus an integral curve in this part of the characteristic surface is a horizontal line $\varphi =$ const., $-u\sin\varphi + v\cos\varphi = 0$. On the contact surface,

$$0 = \mu\,[-\sin\varphi\, du + \cos\varphi\, dv] = d\Phi \,, \tag{B.21}$$

which implies that $\Phi =$ const. along integral curves in this portion. All points on the coincidence locus are critical points for the line field defining integral curves, so that Theorem 4.2 does not apply.

It may be verified that the determinant of Eq. (4.18), which defines the inflection locus, vanishes identically on the contact surface; therefore the eigenvalue corresponding

to this part of the characteristic surface is linearly degenerate. On the ruled surface, the equation for the inflection locus reduces to

$$u\left[\Phi + u\Phi_u + v\Phi_v\right]_u + v\left[\Phi + u\Phi_u + v\Phi_v\right]_v = 0\ , \qquad (B.22)$$

i.e., to the vanishing of the derivative of the eigenvalue along the rarefaction.

In summary, the behavior of rarefactions near the coincidence locus, which separates two regions of strict hyperbolicity, is as follows. A rarefaction curve projected from the contact surface is a level curve Φ = const., whereas a rarefaction curve projected from the ruled surface lies along a line $-u\sin\varphi + v\cos\varphi = 0$, φ = const. The two types of rarefaction curves are tangent to each other at coincidence points, and generically they cross the coincidence locus transversally. The corresponding eigenvalues are $\lambda_{\text{contact}} = \Phi$ and $\lambda_{\text{ruled}} = \Phi + u\Phi_u + v\Phi_v$, respectively. Thus the contact curves are linearly degenerate, while the other eigenvalue typically increases monotonically through the coincidence locus. In particular, λ_{ruled} switches from family 1 to family 2 as the corresponding rarefaction curve is followed, in the direction of increasing eigenvalue, across the coincidence locus; at the same time, λ_{contact} switches from family 2 to family 1.

References

1. A. Azevedo, Thesis, Departamento de Matemática, Pontifícia Universidade Católica do Rio de Janeiro, in preparation, 1988.

2. C. Chicone, "Quadratic Gradients on the Plane are Generically Morse-Smale," *J. Diff. Eq.* **33** (1979), pp. 159–166.

3. C. Chicone and T. Jinghuang, "On General Properties of Quadratic Systems," *Am. Math. Monthly* **89** (1982), pp. 167–178.

4. C. Conley and J. Smoller, "Viscosity Matrices for Two-Dimensional Nonlinear Hyperbolic Systems," *Comm. Pure Appl. Math.* **XXIII** (1970), pp. 867–884.

5. R. Courant and K. Friedrichs, *Supersonic Flow and Shock Waves*, John Wiley, New York, 1948.

6. L. Foy, "Steady State Solutions of Hyperbolic Systems of Conservation Laws with Viscous Terms," *Comm. Pure Appl. Math.* **17** (1964), pp. 177–188.

7. I. Gelfand, "Some Problems in the Theory of Quasi-linear Equations," *Usp. Math. Nauk.* **14** (1959), pp. 87–158. English transl. in Amer. Math. Soc. Transl., Ser. 2, **29** (1963), pp. 295–381.

8. J. Glimm, "Solutions in the Large for Nonlinear Hyperbolic Systems of Equations," *Comm. Pure Appl. Math.* **XVIII** (1965), pp. 697–715.

9. M. E. Gomes, "Singular Riemann Problem for a Fourth-Order Model for Multi-Phase Flow," Thesis (in Portuguese), Departamento de Matemática, Pontifícia Universidade Católica do Rio de Janeiro, 1987.

10. M. E. Gomes, "Riemann Problems Requiring a Viscous Profile Entropy Condition," Preprint, Courant Institute, New York University, 1988.

11. M. E. Gomes, "On Saddle-Saddle Connections in Planar, Quadratic Dynamical Systems," in preparation, 1988.

12. J. Guckenheimer and P. Holmes, *Nonlinear Oscillations, Dynamical Systems, and Bifurcations of Vector Fields*, Springer-Verlag, New York, 1986.

13. H. Holden, "On the Riemann Problem for a Prototype of a Mixed Type Conservation Law," *Comm. Pure Appl. Math.* **XL** (1987), pp. 229–264.

14. H. Holden and L. Holden, "On the Riemann Problem for a Prototype of a Mixed Type Conservation Law, II," Preprint, Univ. of Trondheim, Norway, 1988.

15. E. Hopf, "The Partial Differential Equation $u_t + uu_x = \mu u_{xx}$," *Comm. Pure Appl. Math.* **III** (1950), pp. 201–230.

16. E. Isaacson, "Global Solution of a Riemann Problem for a Nonstrictly Hyperbolic System of Conservation Laws Arising in Enhanced Oil Recovery," *J. Comp. Phys.*, 2001. To appear.

17. E. Isaacson, D. Marchesin, B. Plohr and J. B. Temple, "Multiphase Flow Models with Singular Riemann Problems," Preprint, 1988.

18. E. Isaacson, D. Marchesin, B. Plohr and J. B. Temple, "The Riemann Problem Near a Hyperbolic Singularity: the Classification of Quadratic Riemann Problems I," *SIAM J. Appl. Math.* **48** (1988).

19. E. Isaacson and J. B. Temple, "Examples and Classification of Non-Strictly Hyperbolic Systems of Conservation Laws," *Abstracts of the Amer. Math. Soc.*, January, 1985.

20. E. Isaacson and J. B. Temple, "The Riemann Problem Near a Hyperbolic Singularity II," *SIAM J. Appl. Math.* **48** (1988).

21. E. Isaacson and J. B. Temple, "The Riemann Problem Near a Hyperbolic Singularity III," *SIAM J. Appl. Math.* **48** (1988).

22. E. Isaacson and J. B. Temple, "The Structure of Asymptotic States in a Singular System of Conservation Laws," *Adv. Appl. Math.*, 1988. To appear.

23. B. Keyfitz and H. Kranzer, "A System of Non-Strictly Hyperbolic Conservation Laws Arising in Elasticity Theory," *Arch. Rat. Mech. Anal.* **72** (1980), pp. 219–241.

24. B. Keyfitz and H. Kranzer, "The Riemann Problem for a Class of Hyperbolic Conservation Laws Exhibiting a Parabolic Degeneracy," *J. Diff. Eq.* **47** (1983), pp. 35–65.

25. P. Lax, "Hyperbolic Systems of Conservation Laws II," *Comm. Pure Appl. Math.* **X** (1957), pp. 537–566.

26. T.-P. Liu, "The Riemann Problem for General 2×2 Conservation Laws," *Trans. Amer. Math. Soc.* **199** (1974), pp. 89–112.

27. J. da Mota, "Fundamental Solutions for Thermal Flow of Multiphase Fluids in Porous Media," Thesis (in Portuguese), Departamento de Matemática, Pontifícia Universidade Católica do Rio de Janeiro, 1988.

28. C. F. Palmeira, "Line Fields Defined by Eigenspaces of Derivatives of Maps from the Plane to Itself," Preprint, PUC/RJ, 1987.

29. M. Rascle, "The Riemann Problem for a Nonlinear Non-Strictly Hyperbolic System Arising in Biology," Preprint, Université de Saint-Etienne, 1986.

30. D. Schaeffer and M. Shearer, private communication, 1985.

31. D. Schaeffer and M. Shearer, "The Classification of 2 × 2 Systems of Non-Strictly Hyperbolic Conservation Laws, with Application to Oil Recovery," *Comm. Pure Appl. Math.* **XL** (1987), pp. 141–178.

32. D. Schaeffer and M. Shearer, "Riemann Problems for Nonstrictly Hyperbolic 2 × 2 Systems of Conservation Laws," *Trans. A. M. S.* **304** (1987), pp. 267–306.

33. D. Serre, "Existence Globale de Solutions Faibles sous une Hypothèse Unilaterale," *Q. Appl. Math.* **XLVI** (1988), pp. 157–167.

34. M. Shearer, "The Riemann Problem for 2×2 Systems of Hyperbolic Conservation Laws with Case I Quadratic Nonlinearities," Preprint, North Carolina State University, 1988.

35. M. Shearer, D. Schaeffer, D. Marchesin and P. Paes-Leme, "Solution of the Riemann Problem for a Prototype 2×2 System of Non-Strictly Hyperbolic Conservation Laws," *Arch. Rat. Mech. Anal.* **97** (1987), pp. 299–320.

36. M. Shearer and S. Schecter, "Riemann Problems Involving Undercompressive Shocks," in *Workshop on Partial Differential Equations and Continuum Models of Phase Transitions (Nice, 1988)*, ed. D. Serre, Springer–Verlag, New York, 1988. Lecture Notes in Mathematics.

37. J. B. Temple, "Global Solution of the Cauchy Problem for a Class of 2×2 Non-Strictly Hyperbolic Conservation Laws," *Adv. Appl. Math.* **3** (1982), pp. 335–375.